Data access

Full raw datasets will be shared with researchers upon request. The information of somatic mutations at the respective genomic coordinates has been provided in Table **S2**.

Supporting Information

File S1. Figures S1 to S12 and Tables S3 to S11 are included.
(PDF)

Table S1. The comparison of our dataset with the other different study. We provided the comparison of our dataset with the genes identified in the other different study with transcriptome and epigenome data in lung cancers.
(XLSX)

Table S2. The list of somatic mutations identified from the refined dataset. All mutations described in this table are somatic and non-synonymous mutations.
(XLSX)

Acknowledgements

We thank W. Makałowski for constructive comments and suggestions for this manuscript. We are also grateful to F. Todokoro and F. Iguchi for their technical assistance with the data processing and N. Ogasawara for the Sanger sequencing validation.

Author Contributions

Conceived and designed the experiments: KT YS HE KG SS. Performed the experiments: SM YY AK KM MS. Analyzed the data: AS YS KT. Contributed reagents/materials/analysis tools: KG KT. Wrote the manuscript: AS KT YS.

References

1. The 1000 Genomes Project Consortium (2010) A map of human genome variation from population-scale sequencing. Nature 467: 1061-1073. doi:10.1038/nature09534. PubMed: 20981092.
2. The 1000 Genomes Project Consortium (2012) An integrated map of genetic variation from 1,092 human genomes. Nature 491: 56-65. doi: 10.1038/nature11632. PubMed: 23128226.
3. Choi M, Scholl UI, Ji W, Liu T, Tikhonova IR et al. (2009) Genetic diagnosis by whole exome capture and massively parallel DNA sequencing. Proc Natl Acad Sci U S A 106: 19096-19101. doi:10.1073/pnas.0910672106. PubMed: 19861545.
4. Ng SB, Turner EH, Robertson PD, Flygare SD, Bigham AW et al. (2009) Targeted capture and massively parallel sequencing of 12 human exomes. Nature 461: 272-276. doi:10.1038/nature08250. PubMed: 19684571.
5. Clark MJ, Chen R, Lam HY, Karczewski KJ, Chen R et al. (2011) Performance comparison of exome DNA sequencing technologies. Nat Biotechnol 29: 908-914. doi:10.1038/nbt.1975. PubMed: 21947028.
6. Bamshad MJ, Ng SB, Bigham AW, Tabor HK, Emond MJ et al. (2011) Exome sequencing as a tool for Mendelian disease gene discovery. Nat Rev Genet 12: 745-755. doi:10.1038/nrg3031. PubMed: 21946919.
7. Ng SB, Buckingham KJ, Lee C, Bigham AW, Tabor HK et al. (2010) Exome sequencing identifies the cause of a mendelian disorder. Nat Genet 42: 30-35. doi:10.1038/ng.499. PubMed: 19915526.
8. Biesecker LG (2010) Exome sequencing makes medical genomics a reality. Nat Genet 42: 13-14. doi:10.1038/ng0110-13. PubMed: 20037612.
9. Louis-Dit-Picard H, Barc J, Trujillano D, Miserey-Lenkei S, Bouatia-Naji N et al. (2012) KLHL3 mutations cause familial hyperkalemic hypertension by impairing ion transport in the distal nephron. Nat Genet.
10. Sherry ST, Ward MH, Kholodov M, Baker J, Phan L et al. (2001) dbSNP: the NCBI database of genetic variation. Nucleic Acids Res 29: 308-311. doi:10.1093/nar/29.1.308. PubMed: 11125122.
11. Futreal PA, Coin L, Marshall M, Down T, Hubbard T et al. (2004) A census of human cancer genes. Nat Rev Cancer 4: 177-183. doi: 10.1038/nrc1299. PubMed: 14993899.
12. International Cancer Genome Consortium (2010) International network of cancer genome projects. Nature 464: 993-998. doi:10.1038/nature08987. PubMed: 20393554.
13. Totoki Y, Tatsuno K, Yamamoto S, Arai Y, Hosoda F et al. (2011) High-resolution characterization of a hepatocellular carcinoma genome. Nat Genet 43: 464-469. doi:10.1038/ng.804. PubMed: 21499249.
14. Jones DT, Jäger N, Kool M, Zichner T, Hutter B et al. (2012) Dissecting the genomic complexity underlying medulloblastoma. Nature 488: 100-105. doi:10.1038/nature11284. PubMed: 22832583.
15. The Cancer Genome Atlas Research Network (2011) Integrated genomic analyses of ovarian carcinoma. Nature 474: 609-615. doi: 10.1038/nature10166. PubMed: 21720365.
16. Stephens PJ, Tarpey PS, Davies H, Van Loo P, Greenman C et al. (2012) The landscape of cancer genes and mutational processes in breast cancer. Nature 486: 400-404. PubMed: 22722201.
17. The Cancer Genome Atlas Research Network (2012) Comprehensive genomic characterization of squamous cell lung cancers. Nature.
18. The Cancer Genome Atlas Research Network (2012) Comprehensive molecular characterization of human colon and rectal cancer. Nature 487: 330-337. doi:10.1038/nature11252. PubMed: 22810696.
19. Imielinski M, Berger AH, Hammerman PS, Hernandez B, Pugh TJ et al. (2012) Mapping the hallmarks of lung adenocarcinoma with massively parallel sequencing. Cell 150: 1107-1120. doi:10.1016/j.cell.2012.08.029. PubMed: 22980975.
20. Davies H, Hunter C, Smith R, Stephens P, Greenman C et al. (2005) Somatic mutations of the protein kinase gene family in human lung cancer. Cancer Res 65: 7591-7595. PubMed: 16140923.
21. Ding L, Getz G, Wheeler DA, Mardis ER, McLellan MD et al. (2008) Somatic mutations affect key pathways in lung adenocarcinoma. Nature 455: 1069-1075. doi:10.1038/nature07423. PubMed: 18948947.
22. Kan Z, Jaiswal BS, Stinson J, Janakiraman V, Bhatt D et al. (2010) Diverse somatic mutation patterns and pathway alterations in human cancers. Nature 466: 869-873. doi:10.1038/nature09208. PubMed: 20668451.
23. Forbes SA, Bhamra G, Bamford S, Dawson E, Kok C et al. (2008) The Catalogue of Somatic Mutations in Cancer (COSMIC). Curr Protoc Hum Genet Chapter 10: Unit 10.11: PubMed: 18428421
24. Forbes SA, Bindal N, Bamford S, Cole C, Kok CY et al. (2011) COSMIC: mining complete cancer genomes in the Catalogue of Somatic Mutations in Cancer. Nucleic Acids Res 39: D945-D950. doi: 10.1093/nar/gkq929. PubMed: 20952405.
25. Li H, Durbin R (2009) Fast and accurate short read alignment with Burrows-Wheeler transform. Bioinformatics 25: 1754-1760. doi: 10.1093/bioinformatics/btp324. PubMed: 19451168.
26. McKenna A, Hanna M, Banks E, Sivachenko A, Cibulskis K et al. (2010) The Genome Analysis Toolkit: a MapReduce framework for analyzing next-generation DNA sequencing data. Genome Res 20: 1297-1303. doi:10.1101/gr.107524.110. PubMed: 20644199.
27. DePristo MA, Banks E, Poplin R, Garimella KV, Maguire JR et al. (2011) A framework for variation discovery and genotyping using next-generation DNA sequencing data. Nat Genet 43: 491-498. doi: 10.1038/ng.806. PubMed: 21478889.
28. Welch HC, Coadwell WJ, Ellson CD, Ferguson GJ, Andrews SR et al. (2002) P-Rex1, a PtdIns(3,4,5)P3- and Gbetagamma-regulated guanine-nucleotide exchange factor for Rac. Cell 108: 809-821. doi: 10.1016/S0092-8674(02)00663-3. PubMed: 11955434.

29. Rosenfeldt H, Vázquez-Prado J, Gutkind JS (2004) P-REX2, a novel PI-3-kinase sensitive Rac exchange factor. FEBS Lett 572: 167-171. doi:10.1016/j.febslet.2004.06.097. PubMed: 15304342.
30. Das B, Shu X, Day GJ, Han J, Krishna UM et al. (2000) Control of intramolecular interactions between the pleckstrin homology and Dbl homology domains of Vav and Sos1 regulates Rac binding. J Biol Chem 275: 15074-15081. doi:10.1074/jbc.M907269199. PubMed: 10748082.
31. Hill K, Krugmann S, Andrews SR, Coadwell WJ, Finan P et al. (2005) Regulation of P-Rex1 by phosphatidylinositol (3,4,5)-trisphosphate and Gbetagamma subunits. J Biol Chem 280: 4166-4173. PubMed: 15545267.
32. Chhatriwala MK, Betts L, Worthylake DK, Sondek J (2007) The DH and PH domains of Trio coordinately engage Rho GTPases for their efficient activation. J Mol Biol 368: 1307-1320. doi:10.1016/j.jmb.2007.02.060. PubMed: 17391702.
33. Sosa MS, Lopez-Haber C, Yang C, Wang H, Lemmon MA et al. (2010) Identification of the Rac-GEF P-Rex1 as an essential mediator of ErbB signaling in breast cancer. Mol Cell 40: 877-892. doi:10.1016/j.molcel.2010.11.029. PubMed: 21172654.
34. Kanehisa M, Goto S, Furumichi M, Tanabe M, Hirakawa M (2010) KEGG for representation and analysis of molecular networks involving diseases and drugs. Nucleic Acids Res 38: D355-D360. doi:10.1093/nar/gkp896. PubMed: 19880382.
35. Hecht JL, Mutter GL (2006) Molecular and pathologic aspects of endometrial carcinogenesis. J Clin Oncol 24: 4783-4791. doi:10.1200/JCO.2006.06.7173. PubMed: 17028294.
36. Li C, Fang R, Sun Y, Han X, Li F et al. (2011) Spectrum of oncogenic driver mutations in lung adenocarcinomas from East Asian never smokers. PLOS ONE 6: e28204. doi:10.1371/journal.pone.0028204. PubMed: 22140546.
37. Shigematsu H, Lin L, Takahashi T, Nomura M, Suzuki M et al. (2005) Clinical and biological features associated with epidermal growth factor receptor gene mutations in lung cancers. J Natl Cancer Inst 97: 339-346. doi:10.1093/jnci/dji055. PubMed: 15741570.
38. Sharma SV, Bell DW, Settleman J, Haber DA (2007) Epidermal growth factor receptor mutations in lung cancer. Nat Rev Cancer 7: 169-181. doi:10.1038/nrc2088. PubMed: 17318210.
39. Bos JL (1989) ras oncogenes in human cancer: a review. Cancer Res 49: 4682-4689. PubMed: 2547513.
40. Degen M, Brellier F, Kain R, Ruiz C, Terracciano L et al. (2007) Tenascin-W is a novel marker for activated tumor stroma in low-grade human breast cancer and influences cell behavior. Cancer Res 67: 9169-9179. doi:10.1158/0008-5472.CAN-07-0666. PubMed: 17909022.
41. Degen M, Brellier F, Schenk S, Driscoll R, Zaman K et al. (2008) Tenascin-W, a new marker of cancer stroma, is elevated in sera of colon and breast cancer patients. Int J Cancer 122: 2454-2461. doi:10.1002/ijc.23417. PubMed: 18306355.
42. Brellier F, Martina E, Degen M, Heuzé-Vourc'h N, Petit A et al. (2012) Tenascin-W is a better cancer biomarker than tenascin-C for most human solid tumors. BMC Clin Pathol 12: 14. doi:10.1186/1472-6890-12-14. PubMed: 22947174.
43. Dasika GK, Lin SC, Zhao S, Sung P, Tomkinson A et al. (1999) DNA damage-induced cell cycle checkpoints and DNA strand break repair in development and tumorigenesis. Oncogene 18: 7883-7899. PubMed: 10630641.
44. Bartkova J, Horejsi Z, Koed K, Kramer A, Tort F et al. (2005) DNA damage response as a candidate anti-cancer barrier in early human tumorigenesis. Nature 434: 864-870. doi:10.1038/nature03482. PubMed: 15829956.
45. Yan X, Baxter RC, Firth SM (2010) Involvement of pregnancy-associated plasma protein-A2 in insulin-like growth factor (IGF) binding protein-5 proteolysis during pregnancy: a potential mechanism for increasing IGF bioavailability. J Clin Endocrinol Metab 95: 1412-1420. doi:10.1210/jc.2009-2277. PubMed: 20103653.
46. Overgaard MT, Boldt HB, Laursen LS, Sottrup-Jensen L, Conover CA et al. (2001) Pregnancy-associated plasma protein-A2 (PAPP-A2), a novel insulin-like growth factor-binding protein-5 proteinase. J Biol Chem 276: 21849-21853. doi:10.1074/jbc.M102191200. PubMed: 11264294.
47. Shimasaki S, Shimonaka M, Zhang HP, Ling N (1991) Identification of five different insulin-like growth factor binding proteins (IGFBPs) from adult rat serum and molecular cloning of a novel IGFBP-5 in rat and human. J Biol Chem 266: 10646-10653. PubMed: 1709938.
48. Su Y, Wagner ER, Luo Q, Huang J, Chen L et al. (2011) Insulin-like growth factor binding protein 5 suppresses tumor growth and metastasis of human osteosarcoma. Oncogene 30: 3907-3917. doi:10.1038/onc.2011.97. PubMed: 21460855.
49. Huang T, Jiang M, Kong X, Cai YD (2012) Dysfunctions associated with methylation, microRNA expression and gene expression in lung cancer. PLOS ONE 7: e43441. doi:10.1371/journal.pone.0043441. PubMed: 22912875.
50. Li H, Handsaker B, Wysoker A, Fennell T, Ruan J et al. (2009) The Sequence Alignment/Map format and SAMtools. Bioinformatics 25: 2078-2079. doi:10.1093/bioinformatics/btp352. PubMed: 19505943.
51. Fujimoto A, Nakagawa H, Hosono N, Nakano K, Abe T et al. (2010) Whole-genome sequencing and comprehensive variant analysis of a Japanese individual using massively parallel sequencing. Nat Genet 42: 931-936. doi:10.1038/ng.691. PubMed: 20972442.
52. Quevillon E, Silventoinen V, Pillai S, Harte N, Mulder N et al. (2005) InterProScan: protein domains identifier. Nucleic Acids Res 33: W116-W120. doi:10.1093/nar/gni118. PubMed: 15980438.

Cancer Science
The official journal of the Japanese Cancer Association JCA

Review Article

RET fusion gene: Translation to personalized lung cancer therapy

Takashi Kohno,[1,2,5] Koji Tsuta,[3] Katsuya Tsuchihara,[1] Takashi Nakaoku,[2] Kiyotaka Yoh[4] and Koichi Goto[4]

[1]Division of Translational Research, Exploratory Oncology Research & Clinical Trial Center (EPOC), National Cancer Center, Tokyo; [2]Division of Genome Biology, National Cancer Center Research Institute, Tokyo; [3]Division of Pathology and Clinical Laboratories, National Cancer Center Hospital, Tokyo; [4]Division of Thoracic Oncology, National Cancer Center Hospital East, Kashiwa, Japan

(Received July 2, 2013/Revised July 27, 2013/Accepted August 21, 2013/Accepted manuscript online August 30, 2013/Article first published online October 1, 2013)

Development of lung adenocarcinoma (LADC), the most frequent histological type of lung cancer, depends in many cases on the activation of "driver" oncogenes such as *KRAS*, epidermal growth factor receptor (*EGFR*), and anaplastic lymphoma kinase (*ALK*). Inhibitors that target the EGFR and ALK tyrosine kinases show therapeutic effects against LADCs containing *EGFR* gene mutations and *ALK* gene fusions, respectively. Recently, we and others identified the *RET* fusion gene as a new targetable driver gene in LADC. The RET fusions occur in 1–2% of LADCs. Existing US Food and Drug Administration-approved inhibitors of RET tyrosine kinase show promising therapeutic effects both *in vitro* and *in vivo*, as well as in a few patients. Clinical trials are underway to investigate the therapeutic effects of RET tyrosine kinase inhibitors, such as vandetanib (ZD6474) and cabozantinib (XL184), in patients with *RET* fusion-positive non-small-cell lung cancer. (*Cancer Sci* 2013; 104: 1396–1400)

Personalized Therapy of LADC

Lung cancer is the leading cause of cancer-related mortality worldwide. Lung adenocarcinoma (LADC) is the most frequent type of lung cancer. LADC occurs both in smokers and non-smokers, and its incidence is increasing.[1] Genome analyses of LADC show that these tumors contain distinct genetic alterations that activate oncogenes.[2,3] Genetic alterations that result in the activation of several oncogenes are detected in a mutually exclusive manner (Fig. 1); of the hundreds of genes mutated in each case of LADC, these oncogenes are considered to be "driver genes".[4] Remarkably, molecular targeted therapy using inhibitory drugs against activated oncogene products has begun to replace conventional chemotherapy using cytotoxic drugs, even for first-line use.[2]

The epidermal growth factor receptor (*EGFR*) gene is activated by single amino acid substitution mutations or in-frame amino acid deletion mutations in 10–20% of LADC cases in the USA and in 30–40% of cases in East Asia.[2] Tumors harboring these *EGFR* mutations respond to EGFR tyrosine kinase inhibitors (TKIs) such as erlotinib and gefitinib, thereby improving progression-free survival and quality of life.[5,6] In addition, 3–5% of LADC harbor fusions that result in the activation of the anaplastic lymphoma kinase (*ALK*) gene; such mutations are mutually exclusive with *EGFR* mutations. Inhibitors, such as crizotinib, that target ALK tyrosine kinase show marked therapeutic effects against ALK fusion-positive LADCs.[7–9] These results indicate that personalized therapy for LADC using TKIs selected on the basis of somatic genetic alterations has been realized already; indeed, 20% of USA/European and 40% of Asian LADC patients benefit from such therapies.

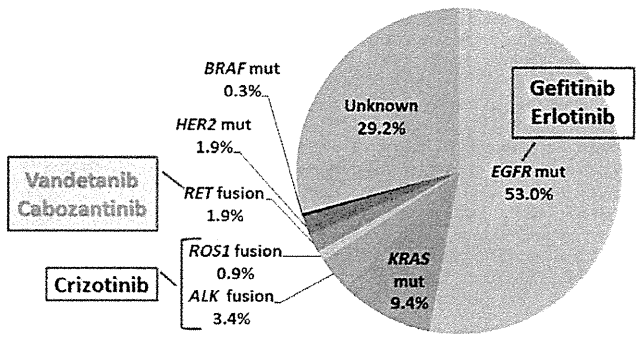

Fig. 1. Pie chart showing the fraction of Japanese lung adenocarcinoma patients that harbor "driver" gene mutations. Surgical specimens from 319 stage I–II lung adenocarcinomas deposited in the National Cancer Center Biobank (Japan) were subjected to analysis. The *EGFR*, *KRAS*, *BRAF*, and *HER2* mutations (mut) were examined using the high resolution melting method, whereas *ALK*, *ROS1* and *RET* fusions were examined by RT-PCR.[12,31] The protocol for this research project has been approved by the institutional review board of the National Cancer Center.

Discovery of the *RET* Fusion Gene as a New Targetable Driver Gene

In 2012, four studies, including one by our group, identified fusions of the *RET* (rearranged during transfection) oncogene[10–13] (Fig. 2). *RET* is a well-known driver oncogene kinase for thyroid cancer, and both activating mutations and fusions of this gene have been observed.[14,15] Germline gain-of-function mutations in *RET* predispose carriers to multiple endocrine neoplasia type 2, which is characterized by medullary thyroid cancer, pheochromocytoma, and hyperparathyroidism, and also to familial medullary thyroid carcinoma syndrome. Somatic gain-of-function *RET* mutations have been observed in 30–50% of sporadic medullary thyroid cancer, and somatic *RET* gene fusions have been observed in 30–50% of sporadic papillary thyroid cancer. The US Food and Drug Administration (FDA) have approved two inhibitory drugs, vandetanib (ZD6474) and cabozantinib (XL184), for the treatment of advanced medullary thyroid cancer. The molecular process for generating a *RET* fusion is similar to the mechanism underlying *ALK* fusion: the most frequent *RET*

[5]To whom correspondence should be addressed.
E-mail: tkkohno@ncc.go.jp

doi: 10.1111/cas.12275

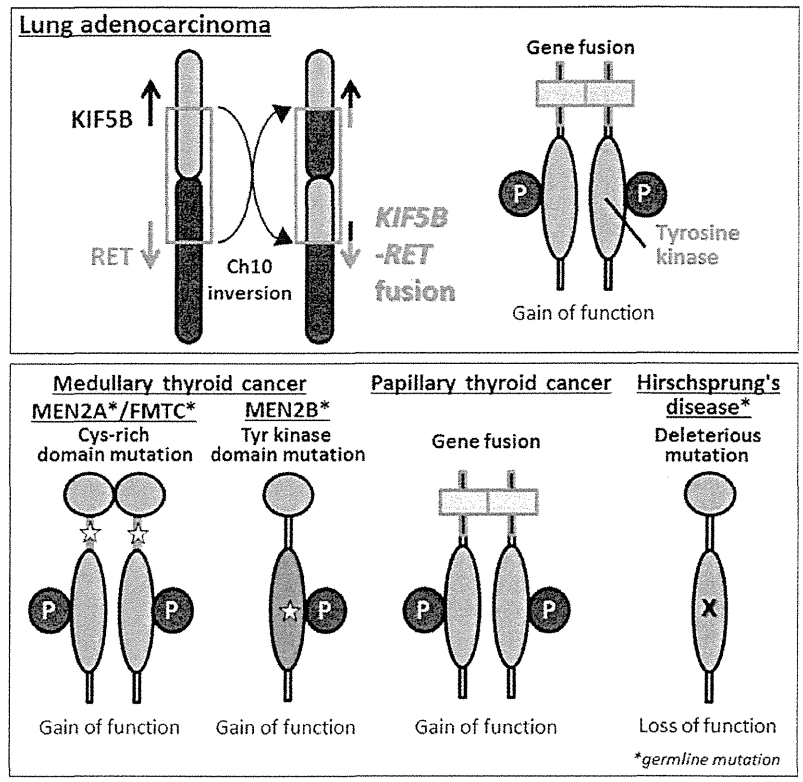

Fig. 2. Involvement of the *RET* gene in lung and thyroid carcinogenesis and in a developmental disorder. Upper panel, somatic inversion in chromosome 10 results in *KIF5B–RET* fusions. The RET fusion protein has constitutive tyrosine (Tyr) kinase activity, representing a gain-of-function alteration. Lower panel, *RET* alterations in other diseases. A germline gain-of-function mutation of *RET* drives thyroid carcinogenesis in patients with multiple endocrine neoplasia type 2 (MEN2). Somatic gain-of-function mutation and translocation of *RET* cause medullary and papillary thyroid cancers, respectively. Germline loss-of-function *RET* mutations cause Hirschsprung's disease, a hereditary disorder characterized by the absence of enteric ganglia in variable segments of intestine. FMTC, familial medullary thyroid carcinoma; P, phosphorylation; X, inactivating mutation.

fusion, *KIF5B–RET*, is generated by a pericentric inversion in chromosome 10, whereas the most frequent *ALK* fusion, *EML4–ALK*, is generated by a paracentric inversion in chromosome 2 (Fig. 2).

Four different strategies resulted in the discovery of the same *RET* fusion gene (Table 1, Fig. 3). We carried out whole-transcriptome sequencing using RNA from 30 snap-frozen surgical LDAC specimens to identify novel fusion-gene transcripts.[12] Ju *et al.*[13] analyzed the whole genome and transcriptome of a single young (33-year-old) LADC patient. Lipson *et al.*[11] carried out targeted-capture sequencing of 145 cancer-relevant genes from genomic DNA obtained from 24 formalin-fixed paraffin-embedded tumor samples to identify genes mutated or fused in LADC. Takeuchi *et al.*[10] carried out a FISH-based screen against known fusion kinase and partner genes to detect rearrangement of oncogenes in >1500 LADC cases.

To date, *RET* fusions have been identified that involve four fusion partners comprising nine subtypes of fusion variants: *KIF5B*, *CCDC6/PTC/H4*, *NCO4/PTC3/ELE1*, and *TRIM33 /PTC7*.[16] The latter three partners are also fused to *RET* in thyroid cancer, whereas *KIF5B* is not. The deduced features of the proteins encoded by all types of *RET* fusion gene are similar to those of ALK: coiled-coil domains in the N-terminal fusion partners cause the RET domains to dimerize, resulting in activation of RET tyrosine kinase in the absence of ligands (Fig. 2). The ligand-independent dimerization and constitutive activation of RET protein are also caused by gain-of-function mutations and translocations of *RET*, which have been detected in sporadic and hereditary thyroid cancers.[15] In fact, autophosphorylation of the KIF5B–RET fusion protein, representing RET protein activation, was observed in LADC tissues harboring the corresponding *RET* fusion gene,[12] as well as in cells cultured in the absence of serum. The transforming and signal-addictive activities of KIF5B–RET fusion proteins are suppressed by FDA-approved drugs (e.g., vandetanib, sorafenib, and sunitinib), which themselves suppress RET kinase.[10–12] In addition, the LADC cell line, LC-2/ad, which harbors a *CCDC6–RET* fusion, is sensitive to these drugs both *in vitro* and *in vivo*.[17,18] Unfortunately, these drugs are not approved for use as treatments for lung cancer; however, the existing data led us to investigate their therapeutic effects in clinical trials, as described below.

Prevalence and Characteristics of *RET* Fusion-Positive LADC

Several studies have validated the presence of *RET* fusion in a small subset of non-small-cell lung cancers (NSCLCs).[16,19–24] The total number of examined cases has reached approximately 5000 (Table 1). Most of the positive cases are LADC, but several cases involve other histological types of NSCLC, such as adenosquamous carcinoma.[19,20] The *RET* fusions are present in 1–2% of NSCLC/ADC of patients of both Asian and European descent. Several studies indicate that *RET* fusion occurs preferentially in young, never-smoker, and light-smoker patients.[10,12,20]

The LADCs harboring *KIF5B–RET* fusions are well or moderately differentiated, similar to LADCs harboring *EGFR* mutations. This is in contrast to *EML4–ALK* fusion-positive LADCs, which tend to show signet-ring and mucinous cribriform patterns.[10] Those LADCs harboring *CCDC6–RET* fusions show such histological features.[10,18]

In our previous study, we did not detect *RET* fusions in a screen of 234 squamous cell, 17 large cell, and 20 small-cell lung cancers.[12] Adenocarcinomas of other organs, such as colon (n = 200) and ovary (n = 100), were also negative for *RET* fusion. To date, whole-transcriptome analysis of other organs has not identified *RET* fusions in cancers outside the lung. Therefore, *RET* fusion may occur mainly in LADC and papillary thyroid cancer.

Table 1. Prevalence of *RET* gene fusion in non-small-cell lung cancer (NSCLC)

Institution	No. of cases examined	No. of *RET* fusion (+) cases	*RET* fusion%	Fusion type	Ref.
	NSCLC/lung adenocarcinoma				
National Cancer Center, Japan	704/433	7/7	1.0/1.6	*KIF5B–RET*: 7	12
Japan Foundation for Cancer Research, Japan	1482/1119	13/13	0.9/1.2	*KIF5B–RET*: 12 *CCDC6–RET*: 1	10
Foundation Med, USA	643/561	12/12	1.8/2.1	*KIF5B–RET*: 12	11
Seoul National University, Korea	21/21 (Driver mutation −)	3/3	14/14	*KIF5B–RET*: 3	13
Chinese Academy of Sciences, China	202/202 (Driver mutation −)	2/2	1.0/1.0	*CCDC6–RET*: 2	24
Nagoya City University, Japan	371/270	3/3	0.8/1.1	*KIF5B–RET*: 3	23
Memorial Sloan-Kettering Cancer Center, USA	69/69 (Driver mutation −)	1/1	1.4/1.4	*KIF5B–RET*: 1	21
Fudan University Shanghai Cancer Center, China	936/633	13/11	1.4/1.7	*KIF5B–RET*: 9 *CCDC6–RET*: 3 *NCOA4–RET*: 1	20
Tongji University School of Medicine, China	392/231	6/4	1.5/1.7	*KIF5B–RET*: 6	19
Korea Research Institute of Bioscience and Biotechnology, Korea	6/6 (Female non-smoker)	1/1	17/17	*CCDC6–RET*: 1	22
Memorial Sloan-Kettering Cancer Center, USA	31/31 (Driver mutation −)	5/5	16/16	*KIF5B–RET*: 2 *TRIM33–RET*: 1 (Unknown: 2)	16
Total	4857/3576	66/62	1.4/1.8	*KIF5B–RET*: 55 *CCDC6–RET*: 7 *NCOA4–RET*: 1 *TRIM33–RET*: 1	

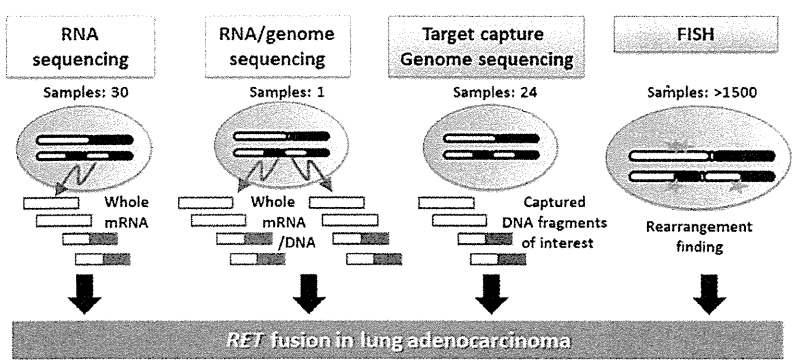

Fig. 3. Strategies used to identify *RET* fusion in lung adenocarcinoma. Four different methods were used to identify novel oncogenic fusions in lung adenocarcinomas.[10–13]

Therapeutic Effects of RET TKIs in Patients with *RET* Fusion-Positive NSCLC

In clinical trials, the ALK TKI, crizotinib, showed a dramatic therapeutic effect against NSCLCs harboring *ALK* gene fusions. Crizotinib was approved for use in the USA in August 2011 and for use in Japan in March 2012.[8] Considering that the *ALK* gene fusion was first identified in NSCLC in 2007, approval has been achieved extremely rapidly. Consequently, the discovery of the *RET* fusion has raised expectations that patients with NSCLCs harboring *RET* fusions will soon benefit from targeted therapy using existing RET TKIs.

Several commercially available multikinase inhibitors, such as vandetanib (ZD6474), cabozantinib (XL184), sorafenib, sunitinib, lenvatinib (E7080), and ponatinib (AP24534), have activity against the RET kinase; however, no selective RET inhibitors have yet been developed for clinical use. Several phase II clinical trials have been initiated to investigate the therapeutic effects of such multikinase inhibitors in patients with advanced *RET* fusion-positive NSCLC (Table 2). As for previous clinical trials of ALK TKIs, all of these trials have open-label and single-arm designs, with response rate as the primary endpoint. One study, carried out by Drilon *et al.* at the Memorial Sloan-Kettering Cancer Center (NCT01639508),

doi: 10.1111/cas.12275

Table 2. Ongoing phase II clinical trials of RET tyrosine kinase inhibitors in patients with *RET* fusion-positive non-small-cell lung carcinoma

Trial number†	Drug (pharmaceutical company)	Study design	Primary end-point	Enrolment no.	Study start
NCT01639508	Cabozantinib/XL184 (Exelixis)			25	July 2012
UMIN000010095	Vandetanib/ZD6474 (AstraZeneca)			17	Feb 2013
NCT01823068	Vandetanib/ZD6474 (AstraZeneca)	Open-label, single arm	Response rate	17	April 2013
NCT01877083	Lenvatinib/E7080 (Eisai)			20	April 2013
NCT01813734	Ponatinib/AP24534 (ARIAD)			20	June 2013

†Detailed information is available at http://clinicaltrials.gov/ or https://upload.umin.ac.jp.

Table 3. Response of lung adenocarcinoma patients to RET tyrosine kinase inhibitors

Patient	*RET* fusion gene	Inhibitor	Ethnicity	Sex	Age, years	Pathological diagnosis	Smoking history (pack-year)	Response (% decrease)	Reference
1	*TRIM33–RET*	Cabozantinib	Caucasian	Female	41	Papillary adenocarcinoma	Never-smoker	Partial response (66)	16
2	*KIF5B–RET*	Cabozantinib	African-American	Female	75	Poorly differentiated adenocarcinoma	Never-smoker	Partial response (32)	16
3	*KIF5B–RET*	Cabozantinib	Caucasian	Female	68	Mixed subtype adenocarcinoma	Never-smoker	Stable disease	16
4	*KIF5B–RET*	Vandetanib	Caucasian	Male	58	Poorly differentiated adenocarcinoma	Former smoker (5)	Decrease in size	26

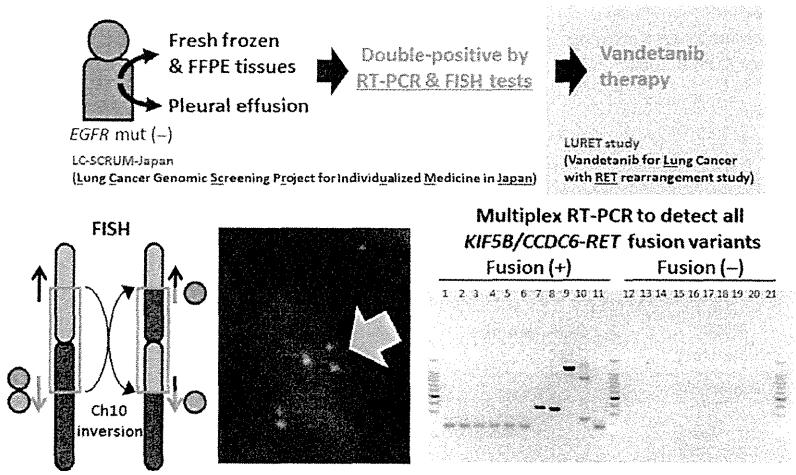

Fig. 4. Consolidated Standards of Reporting Trials diagram of the Lung Cancer Genomic Screening Project for Individualized Medicine in Japan (LC-SCRUM) and the Lung Cancer with *RET* rearrangement (LURET) study in Japan. The LC-SCRUM screen identified 17 *RET* fusion-positive cases from non-squamous non-small-cell lung carcinoma cases without epidermal growth factor receptor (*EGFR*) mutations (mut). The *RET* fusion-positive cases are defined as being positive in both RT-PCR and subsequent FISH tests. Representative pictures of these tests are shown. Fusion-positive cases were treated with vandetanib in the LURET study. Ch10, chromosome 10; FFPE, formalin-fixed paraffin-embedded.

is testing cabozantinib, a drug recently approved by the FDA for the treatment of thyroid cancer. The therapeutic responses of the first three patients to be treated with cabozantinib were reported to be promising (Table 3).[16]

The other phase II clinical trial was initiated by our own group in Japan (UMIN00001009). This trial, designated LURET (Lung Cancer with *RET* rearrangement study), is investigating the therapeutic effects of vandetanib in 17 patients with *RET* fusion-positive NSCLC (Table 2). Because vandetanib is a multikinase inhibitor that is effective against EGFR and vascular endothelial growth factor, this drug was previously examined for its therapeutic efficacy in advanced NSCLC patients in several "all-comer" clinical trials.[25] Those trials were carried out without considering gene alterations in determining eligibility, and the trials did not show significantly greater therapeutic effects than pre-existing therapeutic regimens. Therefore, only *RET* fusion-positive cases, which represent 1–2% of all NSCLCs, are eligible for the LURET study.

To evaluate eligibility for this study, we established a diagnostic method for detecting *RET* fusions using a combination of RT-PCR and FISH (Fig. 4). In this study, RNAs from frozen biopsy tissue or pleural effusion from patients with non-squamous NSCLCs without *EGFR* mutations are subjected to RT-PCR; this method enables us to detect all seven *KIF5B–RET* and *CCDC6–RET* variants identified to date.[16] The positive cases are then subjected to break-apart and fusion FISH to validate the RT-PCR results. Cases positive by both RT-PCR and FISH are eligible for the LURET study. The RT-PCR screening is being carried out in >100 hospitals throughout Japan by a consortium designated LC-SCRUM (Lung Cancer Genomic Screening Project for Individualized Medicine in Japan). The therapeutic results will be obtained within 2 years.

Notably, a recent study reported that one patient with LADC harboring a *KIF5B–RET* fusion responded to vandetanib (Table 3). The patient was Caucasian male and a former smoker. Tumor shrinkage was observed starting in the first week, and continued for 4 weeks.[26]

Perspective

The *RET* gene is predicted to be an additional therapeutic target for therapy against LADC. Three other oncogene kinases,

HER2 (activated by inflame insertion mutations), BRAF (activated by point mutation), and ROS1 (activated by gene fusion) are also promising targets for personalized therapy in addition to EGFR and ALK (Fig. 1). In fact, inhibition of these kinases has yielded therapeutic effects in several lung cancer patients. The LADCs harboring *HER2* mutations responded to therapy with anti-HER2 antibodies and HER2 TKIs.[27] One LADC case harboring a *BRAF* mutation responded to therapy with vemurafenib, an FDA-approved drug for the treatment of melanoma.[28] The ALK TKI, crizotinib, suppresses the activity of the ROS1 tyrosine kinase due to the high structural similarity between the ALK and ROS1 tyrosine kinase domains. Consistent with this, a significant portion of the LADC patients with *ROS1* fusions that were enrolled in a clinical trial responded to crizotinib.[29] Therefore, developing therapies that target RET and other kinases means that increasing numbers of LADC patients will benefit from personalized therapy (Fig. 1). Thus, LADC represents a type of cancer in which "precision cancer medicine"[30] based on somatic gene alterations will be realized.

Acquisition of drug resistance is a serious problem for therapies based on TKIs. The LADCs harboring ALK fusions become resistant to crizotinib by acquiring second-site mutations in the gatekeeper region of ALK tyrosine kinase.[7] Those LADCs harboring *ROS1* fusions also become resistant to crizotinib, in this case through second-site mutations in the gatekeeper region of ROS1.[29] Therefore, *RET* fusion-positive LADCs might also acquire resistance to RET TKIs through the same mechanism. Clinical trials of RET TKIs as a treatment for fusion-positive NSCLCs should be carried out carefully, and focus both on efficacy and the acquisition of resistance.

Acknowledgments

The authors thank all the collaborators in the National Cancer Center and the LC-SCRUM/LURET studies. This work was supported in part by: the Program for Promotion of Fundamental Studies in Health Sciences from the National Institute of Biomedical Innovation; Grants-in-Aid from the Ministry of Health, Labor, and Welfare for the Third-term Comprehensive 10-year Strategy for Cancer Control and for Research on New Drug and Medical Device Development; and the National Cancer Center Research and Development Fund. The National Cancer Center Biobank is supported by the National Cancer Center Research and Development Fund, Japan.

Disclosure Statement

The authors have no conflict of interest.

References

1 Jemal A, Siegel R, Xu J, Ward E. Cancer statistics, 2010. *CA Cancer J Clin* 2010 (Sep–Oct); **60**: 277–300.
2 Oxnard GR, Binder A, Janne PA. New targetable oncogenes in non-small-cell lung cancer. *J Clin Oncol* 2013 (Mar); **31**: 1097–104.
3 Pao W, Hutchinson KE. Chipping away at the lung cancer genome. *Nat Med* 2012 (Mar); **18**: 349–51.
4 Imielinski M. Mapping the hallmarks of lung adenocarcinoma with massively parallel sequencing. *Cell* 2012; **150**: 1107–20.
5 Maemondo M, Inoue A, Kobayashi K *et al.* Gefitinib or chemotherapy for non-small-cell lung cancer with mutated EGFR. *N Engl J Med* 2010 (Jun 24); **362**: 2380–8.
6 Oizumi S, Kobayashi K, Inoue A *et al.* Quality of life with gefitinib in patients with EGFR-mutated non-small cell lung cancer: quality of life analysis of North East Japan Study Group 002 Trial. *Oncologist* 2012; **17**: 863–70.
7 Shaw AT, Engelman JA. ALK in lung cancer: past, present, and future. *J Clin Oncol* 2013 (Mar 10); **31**: 1105–11.
8 Mano H. ALKoma: a cancer subtype with a shared target. *Cancer Discov* 2012 (Jun); **2**: 495–502.
9 Sakamoto H, Tsukaguchi T, Hiroshima S *et al.* CH5424802, a selective ALK inhibitor capable of blocking the resistant gatekeeper mutant. *Cancer Cell* 2011 (May 17); **19**: 679–90.
10 Takeuchi K, Soda M, Togashi Y *et al.* RET, ROS1 and ALK fusions in lung cancer. *Nat Med* 2012 (Mar); **18**: 378–81.
11 Lipson D, Capelletti M, Yelensky R *et al.* Identification of new ALK and RET gene fusions from colorectal and lung cancer biopsies. *Nat Med* 2012 (Mar); **18**: 382–4.
12 Kohno T, Ichikawa H, Totoki Y *et al.* KIF5B-RET fusions in lung adenocarcinoma. *Nat Med* 2012 (Mar); **18**: 375–7.
13 Ju YS, Lee WC, Shin JY *et al.* A transforming KIF5B and RET gene fusion in lung adenocarcinoma revealed from whole-genome and transcriptome sequencing. *Genome Res* 2012 (Mar); **22**: 436–45.
14 Gild ML, Bullock M, Robinson BG, Clifton-Bligh R. Multikinase inhibitors: a new option for the treatment of thyroid cancer. *Nat Rev Endocrinol* 2011 (Oct); **7**: 617–24.
15 Borrello MG, Ardini E, Locati LD, Greco A, Licitra L, Pierotti MA. RET inhibition: implications in cancer therapy. *Expert Opin Ther Targets* 2013 (Apr); **17**: 403–19.
16 Drilon A, Wang L, Hasanovic A *et al.* Response to cabozantinib in patients with RET fusion-positive lung adenocarcinomas. *Cancer Discov* 2013 (Jun); **3**: 630–5.
17 Suzuki M, Makinoshima H, Matsumoto S *et al.* Identification of a lung adenocarcinoma cell line with CCDC6-RET fusion gene and the effect of RET inhibitors in vitro and in vivo. *Cancer Sci* 2013 (Apr 11); **104**: 896–903.
18 Matsubara D, Kanai Y, Ishikawa S *et al.* Identification of CCDC6-RET fusion in the human lung adenocarcinoma cell line, LC-2/ad. *J Thorac Oncol* 2012 (Dec); **7**: 1872–6.
19 Cai W, Su C, Li X *et al.* KIF5B-RET fusions in Chinese patients with non-small cell lung cancer. *Cancer* 2013 (Apr 15); **119**: 1486–94.
20 Wang R, Hu H, Pan Y *et al.* RET fusions define a unique molecular and clinicopathologic subtype of non-small-cell lung cancer. *J Clin Oncol* 2012 (Dec 10); **30**: 4352–9.
21 Suehara Y, Arcila M, Wang L *et al.* Identification of KIF5B-RET and GOPC-ROS1 fusions in lung adenocarcinomas through a comprehensive mRNA-based screen for tyrosine kinase fusions. *Clin Cancer Res* 2012 (Dec 15); **18**: 6599–608.
22 Kim SC, Jung Y, Park J *et al.* A high-dimensional, deep-sequencing study of lung adenocarcinoma in female never-smokers. *PLoS ONE* 2013; **8**: e55596.
23 Yokota K, Sasaki H, Okuda K *et al.* KIF5B/RET fusion gene in surgically-treated adenocarcinoma of the lung. *Oncol Rep* 2012 (Oct); **28**: 1187–92.
24 Li F, Feng Y, Fang R *et al.* Identification of RET gene fusion by exon array analyses in "pan-negative" lung cancer from never smokers. *Cell Res* 2012 (May); **22**: 928–31.
25 Chu CT, Sada YH, Kim ES. Vandetanib for the treatment of lung cancer. *Expert Opin Investig Drugs* 2012 (Aug); **21**: 1211–21.
26 Gautschi O, Zander T, Keller FA *et al.* A patient with lung adenocarcinoma and RET fusion treated with vandetanib. *J Thorac Oncol* 2013 (May); **8**(5): e43–4.
27 Mazieres J, Peters S, Lepage B *et al.* Lung cancer that Harbors an HER2 mutation: epidemiologic characteristics and therapeutic perspectives. *J Clin Oncol* 2013 (Jun 1); **31**: 1997–2003.
28 Gautschi O, Pauli C, Strobel K *et al.* A patient with BRAF V600E lung adenocarcinoma responding to vemurafenib. *J Thorac Oncol* 2012 (Oct); **7**(10): e23–4.
29 Awad MM, Katayama R, McTigue M *et al.* Acquired resistance to crizotinib from a mutation in CD74-ROS1. *N Engl J Med* 2013 (Jun 1); **368**: 2395–401.
30 Mendelsohn J. Personalizing oncology: perspectives and prospects. *J Clin Oncol* 2013 (May 20); **31**: 1904–11.
31 Yoshida A, Kohno T, Tsuta K *et al.* ROS1-rearranged lung cancer: a clinicopathologic and molecular study of 15 surgical cases. *Am J Surg Pathol* 2013 (Apr); **37**: 554–62.

doi: 10.1111/cas.12275

MODERN PATHOLOGY (2013), 1–10

Immunohistochemical detection of ROS1 is useful for identifying *ROS1* rearrangements in lung cancers

Akihiko Yoshida[1], Koji Tsuta[1], Susumu Wakai[1], Yasuhito Arai[2], Hisao Asamura[3], Tatsuhiro Shibata[2], Koh Furuta[1], Takashi Kohno[4] and Ryoji Kushima[1]

[1]*Division of Pathology and Clinical Laboratories, National Cancer Center Hospital, Tokyo, Japan;* [2]*Division of Cancer Genomics, Center for Medical Genomics, National Cancer Center Research Institute, Tokyo, Japan;* [3]*Division of Thoracic Surgery, National Cancer Center Hospital, Tokyo, Japan and* [4]*Division of Genome Biology, National Cancer Center Research Institute, Tokyo, Japan*

The recent discovery and characterization of an oncogenic *ROS1* gene fusion in a subset of lung cancers has raised significant clinical interest because small molecule inhibitors may be effective to these tumors. As lung cancers with *ROS1* rearrangements comprise only 1–3% of lung adenocarcinomas, patients with such tumors must be identified to gain optimal benefit from molecular therapy. Recently, immunohistochemical analyses using a novel anti-ROS1 rabbit monoclonal antibody (D4D6) have shown promise for accurate identification of *ROS1*-rearranged cancers. To validate this finding, we compared the immunostaining results of tissue microarrays (TMAs) containing 17 *ROS1*-rearranged and 253 *ROS1*-non-rearranged lung carcinomas. All 17 *ROS1*-rearranged cancers showed ROS1 immunoreactivity mostly in a diffuse and moderate-to-strong manner with an H-score range of 5–300 (median, 260). In contrast, 69% of *ROS1*-non-rearranged cancers lacked detectable immunoreactivity, whereas the remaining 31% showed reactivity mainly in a weak or focal manner. The H-score for the entire *ROS1*-non-rearranged group ranged from 0 to 240 (median, 0). The difference in H-score between the two cohorts was statistically significant, and the H-score cutoff (≥150) allowed optimal discrimination (94% sensitivity and 98% specificity). Similar but slightly less-specific performance was achieved using the extent of diffuse (≥75%) staining or ≥2+ staining intensity as cutoffs. *CD74-ROS1* and *EZR-ROS1* fusions were significantly associated with at least focal globular immunoreactivity and plasma membranous accentuation, respectively, and these patterns were specific to *ROS1*-rearranged cases. Although full-length ROS1 is expressed in some *ROS1*-non-rearranged cases, we showed that establishment of an optimal set of interpretative criteria makes ROS1 immunohistochemistry a valuable method to rapidly and accurately screen lung cancer patients for appropriate molecular therapy.
Modern Pathology advance online publication, 1 November 2013; doi:10.1038/modpathol.2013.192

Keywords: adenocarcinoma; immunohistochemistry; lung; ROS1

A significant proportion of lung carcinomas are not amenable to surgical management because they present at advanced stages or recur after primary resection.[1] Molecular subclassification of tumors is particularly important for such cases because genetic change is the major determinant of the effectiveness of targeted molecular therapy. For example, lung cancers with anaplastic lymphoma kinase (*ALK*) gene rearrangements are susceptible to treatment with ALK inhibitors (for example, crizotinib),[2] and those with a mutation in the gene encoding epidermal growth factor receptor (*EGFR*) respond to EGFR inhibitors (for example, erlotinib and gefitinib).[3] The recent discovery and characterization of oncogenic *ROS1* gene fusion in lung adenocarcinomas[4–8] have expanded the list of the molecular subsets of lung cancers. *ROS1* encodes a protein tyrosine kinase that belongs to the insulin receptor family. *ROS1* is fused to one of a number of genes in lung cancers, including *CD74, SLC34A2, EZR, LRIG3, SDC4, TPM3, FIG* (also known as *GOPC*), *CCDC6*, and *KDELR2*.[4–7,9–12] In these fusions, the 3′ region of *ROS1* encoding its kinase

Correspondence: Dr A Yoshida, MD, PhD, Department of Pathology and Clinical Laboratories, National Cancer Center Hospital, 5-1-1 Tsukiji, Chuo-ku, Tokyo 104-0045, Japan.
E-mail: akyoshid@ncc.go.jp
Received 5 July 2013; accepted 2 September 2013; published online 1 November 2013

domain is fused to the 5′ region of the respective partner gene. The fusion encodes a chimeric protein with constitutive kinase activity that initiates oncogenic intracellular signal transduction cascades.[7,13] Preclinical data suggest that *ROS1*-rearranged cancers respond to ALK inhibitors,[5,6,9] and a recent clinical trial[14] revealed a marked inhibition of this molecular subclass by crizotinib. These data underscore the clinical importance of identifying *ROS1*-rearranged cancers to customize treatment.

As *ROS1*-rearranged lung cancer comprises only 1–3% of lung adenocarcinomas,[4–9,15] the appropriate patients must be selected who will benefit most from molecular therapy. Although these cancers are diagnosed using the reverse transcriptase-polymerase chain reaction (RT-PCR) and/or fluorescence *in situ* hybridization (FISH), molecular assays are time-consuming, costly, and not suitable for rapid screening. Unfortunately, clinicopathologic features serve poorly for this purpose. Although *ROS1*-rearranged cancer tends to occur in young non-smokers,[5,7,8] clinical parameters are not sufficiently predictive for successful triage. Similarly, although the characteristic histological features have been described for this subset,[7,8] their role is likely limited in the care of patients who present at advanced stages where molecular therapy is most needed because such features are present in only a subset of fusion-positive cases typically as a focal manner.[8] Recently, Rimkunas *et al*[9] developed a novel anti-ROS1 rabbit monoclonal antibody (D4D6) and proposed the utility of immunohistochemistry for identifying *ROS1*-rearranged cancers by showing its 100% (8/8) sensitivity and 100% (138/138) specificity when compared with break-apart FISH. However, the issue is still controversial because other investigators[16,17] observed *ROS1* expression in a significant proportion (20–30%) of lung carcinomas likely unassociated with gene rearrangement. In this study, we applied this D4D6 antibody to a large number of lung cancers with a known *ROS1* rearrangement status to test the utility of immunohistochemistry for molecular subtyping.

Materials and methods

Case Selection

After receiving approval from the institutional review board at the National Cancer Center in Tokyo, we constructed TMAs containing 346 primary lung adenocarcinomas by using a tissue-arraying instrument (Azumaya, Tokyo, Japan). The tumors were collected from surgical resections with curative intent performed at the National Cancer Center Hospital from 1997 to 2009, and they were enriched for *EGFR* wild-type cases by using high-resolution melting analysis[18] (27% were *EGFR* mutants). Each tumor was sampled by collecting 2.0-mm-diameter cores from two different representative sites. The TMAs were analyzed by using *ROS1* break-apart FISH as described below. After exclusion of 84 cases that either failed to hybridize or lacked an adequate amount of evaluable tumor tissue in the cores, 9 *ROS1*-rearranged cases and 253 *ROS1*-non-rearranged cases were identified. The ranges of rearrangement-positive cell rate in the *ROS1*-rearranged and *ROS1*-non-rearranged cohorts were 42–84% and 0 – 8%, respectively; no case showed borderline 10 – 20% range of rearrangement signals. To expand the rearrangement-positive cohort, eight *ROS1*-rearranged tumors (seven adenocarcinomas and one adenosquamous carcinoma) that were separately identified using RT-PCR were also included, and they were similarly assembled in a TMA as duplicate 2.0-mm cores, except for one case with a limited amount of tissue. Of the 17 *ROS*-rearranged cancers included in this study, 15 were previously reported with their detailed clinicopathologic findings.[8]

FISH

FISH assays were performed using a custom *ROS1* break-apart probe set (Chromosome Science Labo Inc., Sapporo, Japan), which hybridizes with the neighboring 5′ telomeric (RP11-48A22, labeled with SpectrumGreen) and 3′ centromeric (RP11-1036C2, labeled with SpectrumOrange) sequence of the *ROS1* gene. This probe set is designed to detect all known *ROS1* fusions, including *FIG–ROS1*, which is unlikely to be detected using a previously described design[5,8] in which the 5′ probe hybridizes with the RP11-835I21 region. The present probe was internally validated to identify the *FIG–ROS1* fusion in the U-118 MG glioblastoma cell line.[19] FISH images were captured using the Metafer Slide Scanning Platform (MetaSystems, Altlussheim, Germany) to facilitate analysis. Fifty non-overlapping tumor cells with at least one each of 5′ and 3′ signals were examined for each case. The rearrangement-positive cells were defined as those with split signals or isolated red (3′) signals. The specimen was considered as *ROS1*-rearranged if the rearrangement-positive cells constituted $\geq$15% of the enumerated tumor cells. This 15% cutoff value was previously established to accurately differentiate between *ROS1*-rearranged and *ROS1*-non-rearranged cases based on RT-PCR data.[8]

Multiplex RT-PCR

Multiplex RT-PCR was performed as described previously[8] and was designed to detect the fusion transcripts as follows: *CD74-ROS1*, *EZR-ROS1*, *SLC34A2-ROS1*, *FIG–ROS1*, *LRIG3-ROS1*, *SDC4-ROS1*, and *TPM3-ROS1*. The PCR products were subjected to Sanger sequencing.

ROS1 Immunohistochemistry

Immunohistochemical staining was performed on TMA sections, except for one *ROS1*-rearranged case that was evaluated using the whole section. Four-micrometer-thick sections were deparaffinized, and heat-induced epitope retrieval was performed with targeted retrieval solution (pH 9) (Dako, Carpinteria, CA, USA). The slides were treated with 3% hydrogen peroxide for 20 min to block endogenous peroxidase activity. The slides were then incubated with a primary antibody against ROS1 (D4D6, 1:100, Cell Signaling Technology, Danvers, MA, USA) at 4 °C overnight. Reactivity was detected using the EnVision-FLEX+ (Dako). Immunostained slides were scored using the H-score method, which is based on the percentages of cells stained with intensities of 0, 1+, 2+, and 3+ as follows: H-score = $\sum$ [intensity (0, 1, 2, 3) × extent of each staining intensity (%)]. H-scores range from 0 to 300. Intensity 0 was defined as no detectable staining. Intensity 1+ was defined as reactivity only detectable at high magnification (× 20 – 40 objective). More intense reactivity was divided into moderate (2+) and strong (3+) based on the ease of detection at low magnification (× 4 objective).

Statistical Analysis

All data were analyzed using SPSS version 20.0 (IBM Corporation, Somers, NY, USA). The Fisher's exact test and the Mann–Whitney *U*-test were used for categorical and continuous data, respectively. *P*-values were two-tailed, and $P<0.05$ was considered significant.

Results

Immunohistochemical Analysis of ROS1 Expression

Immunostaining was evaluated based on the results of two TMA cores for each tumor, except for 12 *ROS1*-non-rearranged cases for which scoring was performed on one core that contained tumor tissue. All 17 *ROS1*-rearranged cancers showed ROS1 immunoreactivity primarily in a diffuse and moderate-to-strong manner with an H-score range of 5–300 (median, 260, Figure 1a). In contrast, most (69%) *ROS1*-non-rearranged cancers lacked detectable immunoreactivity (Figure 1b), whereas the remaining 31% showed some degree of reactivity, mostly in a weak or focal manner (Figure 1c). The H-score for the entire *ROS1*-non-rearranged group ranged from 0 to 240 (median, 0). The difference in H-score between the two cohorts was statistically significant ($P<0.001$). The staining pattern in all the 95 immunopositive cases (17 *ROS1*-rearranged and 78 *ROS1*-non-rearranged cases) was cytoplasmic. The background lung parenchyma included in the TMA cores occasionally showed ROS1 staining in macrophages (14 cases) and in reactive type II pneumocytes (15 cases, Figure 1d).

Establishment of Immunostaining Interpretative Criteria to Predict Gene Rearrangement

The distribution of H-scores is illustrated in Figure 2. As the scores were continuous rather than sharply separated into two categories, we attempted to establish an optimal set of criteria that helps to predict *ROS1* rearrangement. As there is no universally accepted H-score as a cutoff in the literature, we set a range of H-scores (0, 5, 10, 20, 50, 100, 150, 200, and 250) as the cutoff and calculated test sensitivity and specificity for each condition. This analysis showed that an H-score of ≥150 best discriminated between *ROS1*-rearranged and -non-rearranged cases with 94% sensitivity and 98% specificity (Table 1). Moreover, we set an array of more conventional criteria based on staining extent or intensity and similarly calculated test sensitivity and specificity for each condition. The best separation was achieved when immunopositivity was defined as ≥75% tumor cells labeling with any intensity, and it produced 94% sensitivity and 90% specificity (Table 1). Similar results (94% sensitivity and 87% specificity) were obtained when the immunopositivity was defined as ≥2+ intensity in any extent.

Correlation of ROS1 Fusion Partner With Staining Pattern

Among 17 rearrangement-positive cases, data on *ROS1* fusion partners were available for 15 cases as follows: *CD74-ROS1* (C6;R34), $n=10$; *EZR-ROS1* (E10;R34), $n=4$; *SLC34A2-ROS1* (S13del2046;R34), $n=1$. Among 10 *CD74-ROS1*-positive tumors, six showed at least focal globular immunoreactivity, comprising 1–6 round to ovoid intense intracytoplasmic signals measuring 3–8 μm in diameter. These globules appeared randomly distributed within the cytoplasm rather than restricted to the perinuclear zones. They occurred within the background of weaker cytoplasmic staining and were occasionally associated with adjacent fine granularity. This pattern was observed in almost all cells in one case (Figure 3a), whereas it was observed in a subset of cells in the remaining five cases (Figure 3b). This pattern was not observed in the remaining four *CD74-ROS1*-positive tumors and five *ROS1*-rearranged tumors with partners other than *CD74*. The association between a globular pattern and *CD74* as a fusion partner was statistically significant ($P=0.044$). One tumor (P16) that was not subjected to RT-PCR also showed this globular pattern.

Among the four *EZR-ROS1*-positive tumors, three showed at least focal plasma membranous linear accentuation with occasional fine granular quality.

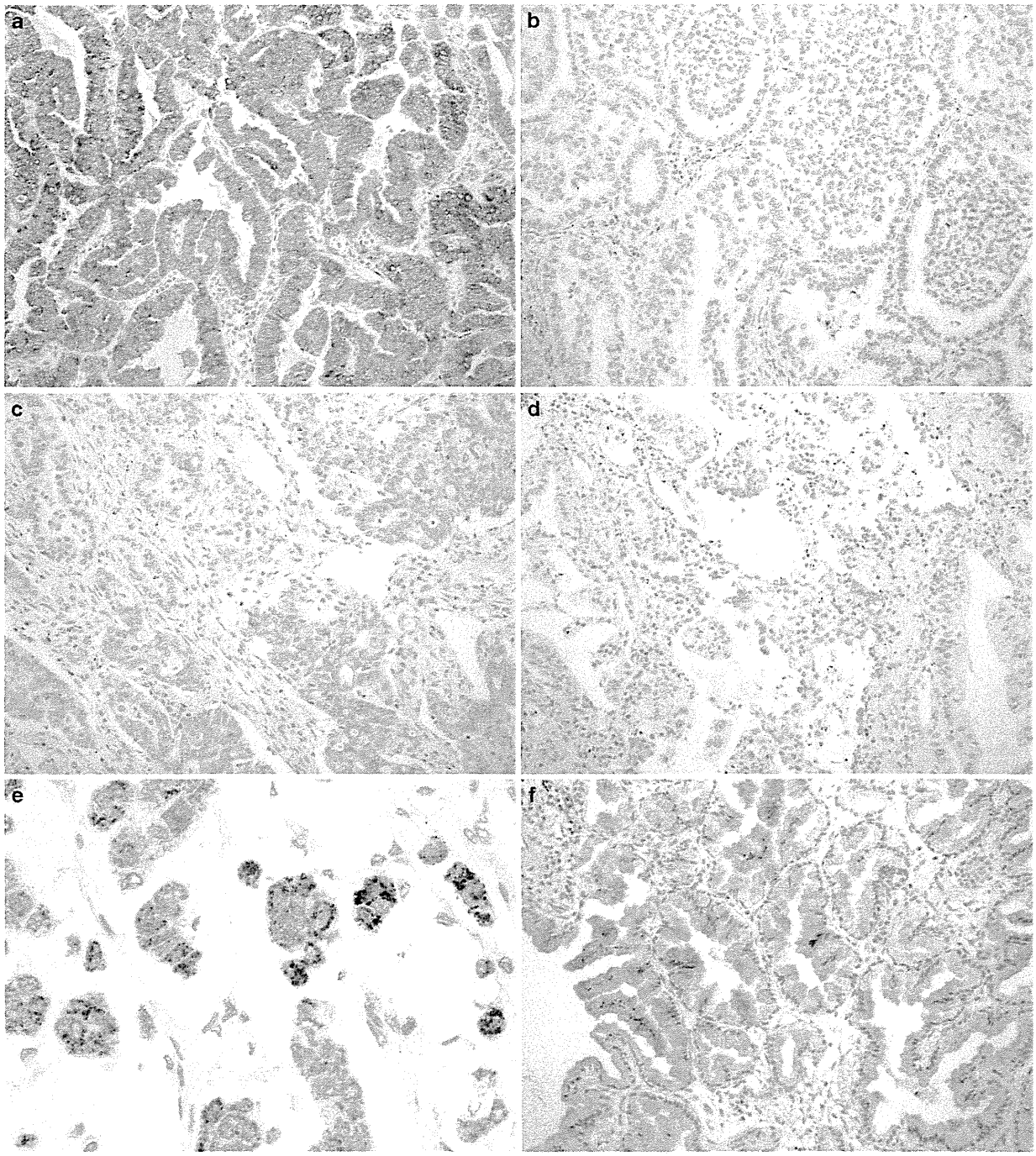

Figure 1 Most *ROS1*-rearranged cancers showed diffuse and moderate-to-strong ROS1 immunoreactivity (**a**), whereas 69% of *ROS1*-non-rearranged cancers lacked detectable ROS1 expression (**b**). The remaining 31% of *ROS1*-non-rearranged cancers expressed ROS1, mainly in a weak or focal manner (**c**). Adjacent lung parenchyma showed occasional ROS1 expression in reactive type II pneumocytes (**d**). The pattern of ROS1 reactivity in some *ROS1*-non-rearranged tumors was distinctly granular (**e**). The majority of invasive mucinous adenocarcinomas showed ROS1 reactivity despite the lack of a gene rearrangement (**f**).

Memebranous accentuation appeared on the lateral surface of tumor cells in two cases (Figure 3c) and along the apical surface in one case (Figure 3d). This pattern was not observed in the remaining *EZR-ROS1*-positive tumor and 11 *ROS1*-rearranged tumors with partners other than *EZR*. The association between membranous accentuation and *EZR* as a fusion partner was statistically significant ($P=0.009$). None of the 78 rearrangement-negative tumors with ROS1 expression showed globular

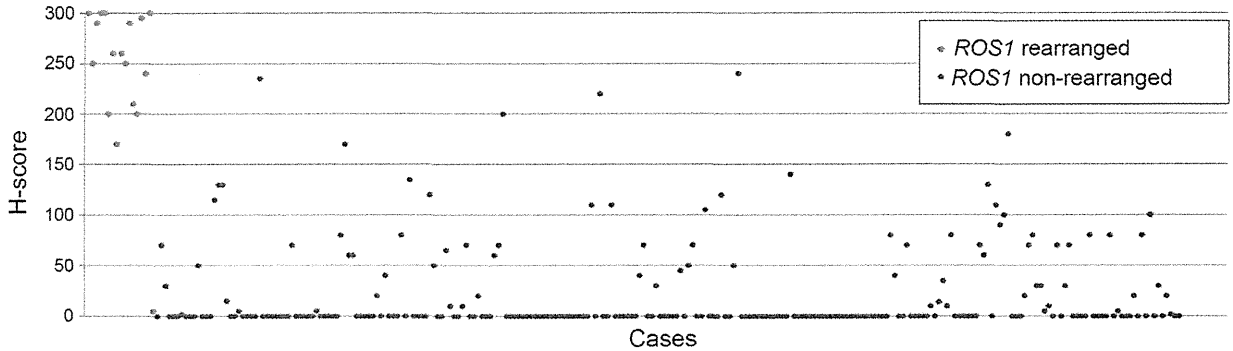

Figure 2 Distribution of H-scores for lung adenocarcinomas determined by using ROS1 immunohistochemistry. Red dots represent scores of *ROS1*-rearranged cases, and blue dots represent scores of *ROS1*-non-rearranged cases.

Table 1 Performance of ROS1 immunohistochemical analysis to predict *ROS1* rearrangement using an array of interpretative criteria

Criteria	*The number of ROS1-rearranged cases that meet the criteria (total N = 17)*	*The number of ROS1-non-rearranged cases that meet the criteria (total N = 253)*	*Sensitivity*	*Specificity*
H-score				
H-score >0	17	78	100%	69%
H-score ≥5	17	76	100%	70%
H-score ≥10	16	72	94%	72%
H-score ≥20	16	65	94%	74%
H-score ≥50	16	49	94%	81%
H-score ≥100	16	20	94%	92%
H-score ≥150[a]	16	6	94%	98%
H-score ≥200	15	4	88%	98%
H-score ≥250	12	0	71%	100%
Extent				
Extent ≥1%	17	78	100%	69%
Extent ≥5%	17	76	100%	70%
Extent ≥10%	16	70	94%	72%
Extent ≥50%	16	48	94%	81%
Extent ≥75%[a]	16	25	94%	90%
Extent = 100%	15	6	88%	98%
Intensity				
Intensity ≥2+[a]	16	33	94%	87%
Intensity = 3+	13	8	76%	97%

[a]Indicates optimal criteria to predict *ROS1* rearrangement.

reactivity or plasma membranous accentuation. The only *SLC34A2-ROS1*-positive case showed solid cytoplasmic ROS1 staining without distinctive features.

Analysis of Immunopositive ROS1-Non-Rearranged Cases

Among the 78 immunopositive *ROS1*-non-rearranged cases, 16 (21%) showed at least focal granular-staining quality (Figure 1e), and the remaining 62 cases (79%) showed non-granular solid staining. Twelve tumors (15%) were morphologically classified as invasive mucinous adenocarcinoma (formerly mucinous bronchioloalveolar carcinoma with invasion;[20] Figure 1f). They comprised 80% of the 15 invasive mucinous adenocarcinomas included here. Among the remaining 238 non-mucinous *ROS1*-non-rearranged cases, we did not observe a clear correlation between histology and immunoreactivity.

Analysis of ROS1-Rearranged Cases with Low Immunostaining

Two *ROS1*-rearranged tumors exhibited less ROS1 staining than did the other 15 cases. One (P8) was an adenocarcinoma that was almost purely composed of signet-ring cells (Figure 4a) whose *ROS1* rearrangement (*EZR-ROS*) was confirmed using FISH and RT-PCR. The tumor showed diffuse but weak to moderate ROS1 reactivity with an H-score of 170 (Figure 4b). The other outlier case (P17) was an adenocarcinoma resected from a non-smoking Japanese woman in her 50's. It was positive for FISH with 78% of tumor cells having rearrangement patterns mostly in the form of isolated 3′ signals (Figure 5a). FISH positivity was confirmed by examining multiple microscopic fields and by using a probe set of different design (RP11-1036C2 for the 3′ probe and RP11-835I21 for the 5′ probe). However, this case showed only weak focal staining with an H-score of 5 (Figure 5b), and this modest reactivity was confirmed using the whole section. Interestingly, multiplex RT-PCR using fresh frozen material did not detect an *ROS1* fusion transcript. Further, this case harbored a deletion of *EGFR* exon 19 and showed diffuse strong immunoreactivity, detected by using an EGFR deletion (E746-A750del)-specific antibody (clone 6B6, 1:100, Cell Signaling Technology) (Figure 5c). As the disease was in the early stage, the patient was successfully treated by surgical resection and did not undergo molecular-targeted therapy.

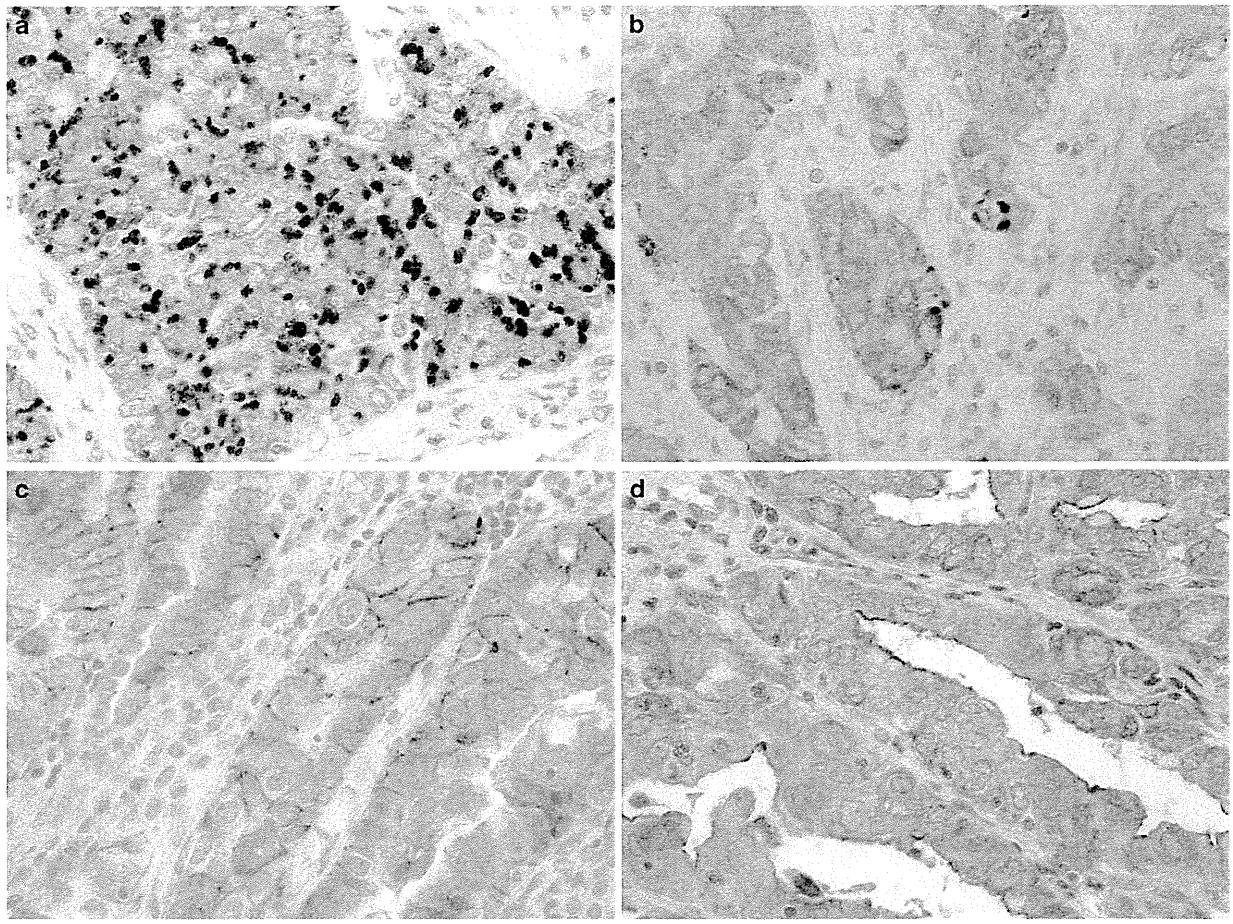

Figure 3 The *ROS1* fusion partner correlated with the ROS1-staining pattern. Diffuse (**a**) or focal (**b**) intracytoplasmic globular reactivity was observed in 6 of 10 *CD74-ROS1*-positive cancers. Plasma membranous accentuation with a fine granular quality was observed in 3 of 4 *EZR-ROS1*-positive tumors; reactivity localizes to the lateral surface in two cases (**c**) and along the apical surface in one case (**d**).

Discussion

We showed here that ROS1 immunoreactivity significantly differed between *ROS1*-rearranged and -non-rearranged lung adenocarcinoma cohorts. However, unlike the observation by Rimkunas *et al*,[9] the reactivity in our present study did not separate the cases into two discrete categories that were in perfect concordance with rearrangement status. In contrast, it produced continuous scores that required statistical treatment for practical application. The reason for this discrepancy may be attributed to the technical differences and the difference in the size of the cases. Our finding of ROS1 expression in 31% of *ROS1*-non-rearranged tumors agrees with those of others. For example, in microarray analyses, *ROS1* mRNA level was significantly elevated in 20–30% of non-small cell lung cancers,[16] and one study[15] specifically documented the *ROS1* mRNA expression independent of gene rearrangement. Similarly, immunohistochemical analyses by Lee *et al*[17] found that 22% of non-small cell lung carcinomas expressed ROS1. Taken together, these data highlight the importance of establishing the optimal immunostaining interpretative criteria to predict gene rearrangement.

In our search for such criteria, we found that an H-score of 150 was a reasonable cutoff because of its 94% sensitivity and 98% specificity. However, H-score-based criteria may not be practical because H-scores are not routinely used in diagnosis. We therefore tested more conventional sets of criteria that are readily applicable to practice and achieved an optimal test performance (94% sensitivity and 90% specificity) by using diffuse ($\geq$75%) staining of any intensity to define a positive result. Although we noted similar performance using $\geq$2+ staining intensity, intensity is relatively subjective and is likely more dependent on the staining protocol. In this regard, a previous study[9] showed 1+ staining intensity in one-third of the *ROS1*-rearranged tumors tested, although it did not document the extent of reactivity.[9] The use of diffuse staining as a criterion to indicate gene rearrangement is reasonable because *ROS1* rearrangement is diffusely present within a tumor,[8] as is typical of early driver

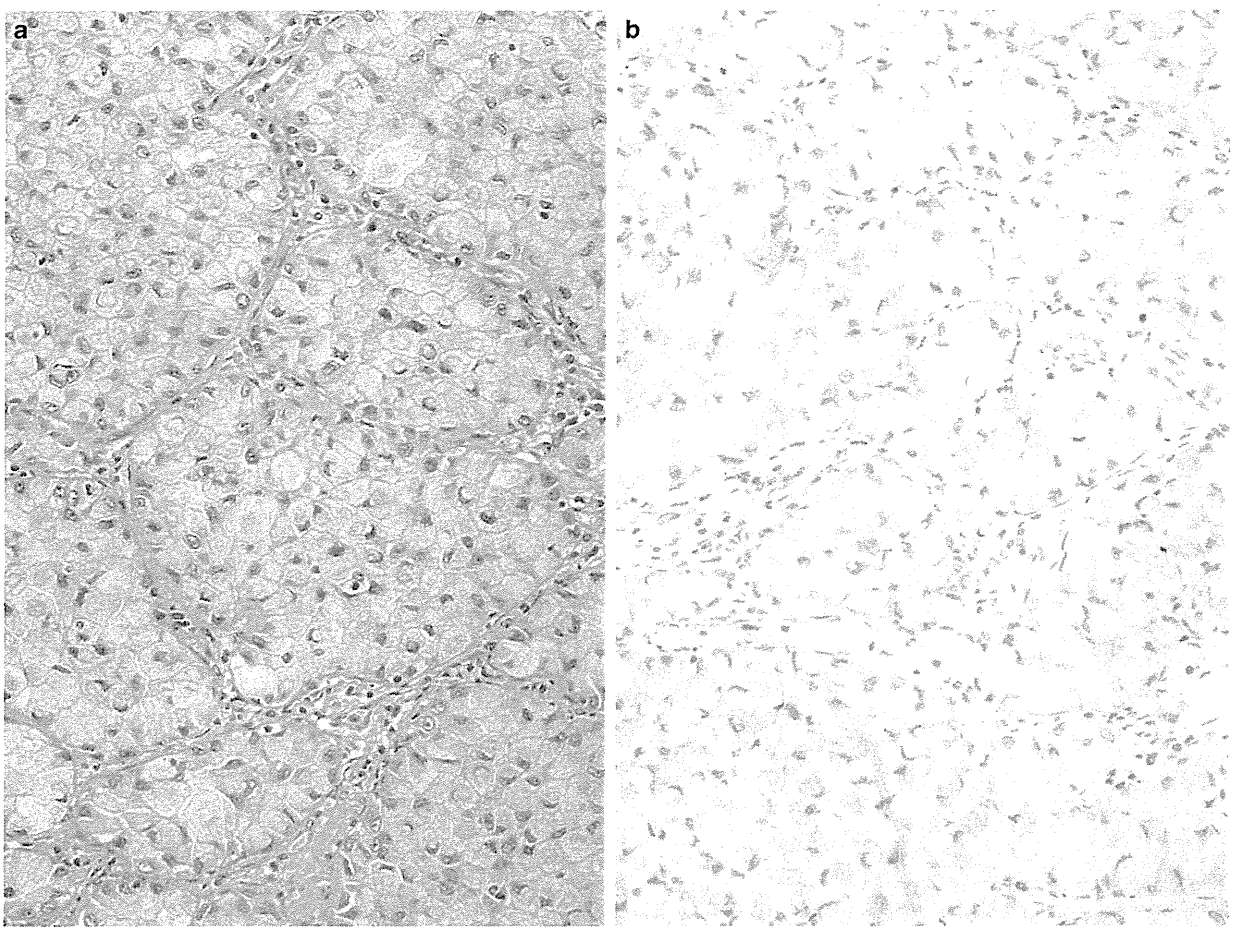

Figure 4 One *EZR-ROS1*-positive signet-ring cell carcinoma (**a**) showed diffuse but only weak–moderate ROS1 immunoreactivity (**b**).

genetic changes such as *ALK* rearrangement[21]and *EGFR* mutation.[22]

We noted a correlation between *ROS1* fusion partner genes and the staining patterns, and the result requires validation using a larger cohort. *CD74-ROS1* was significantly associated with at least focal globular immunoreactivity. This pattern probably corresponds to the intracytoplasmic puncta that Rimkunas *et al*[9] documented in two of the four *CD74-ROS1*-positive lung cancers. The mechanism that generates this unusual staining pattern is unknown but may be related to the physiological localization of the CD74 protein that chaperones MHC class II through the intracellular membrane system.[23] Similarly, the plasma membranous accentuation of reactivity associated with *EZR-ROS1* may reflect the subcellular distribution of ezrin protein that links the plasma membrane with the actin cytoskeleton.[24] These characteristic ROS1-staining patterns were not observed in the 78 rearrangement-negative ROS1-expressing cancers in our cohort and, thus, they may be viewed as a rearrangement-specific phenomenon that can be useful for screening. However, we caution that their recognition may not be straightforward because these patterns may be observed only in a fraction of tumor cells (Figure 3b) and because some *ROS1*-non-rearranged tumors may show at least focal granular staining quality that must be distinguished from CD74-associated globular appearance (compare Figures 1e and 3a).

Our detailed histological analysis of immunohistochemically 'false-positive' cases revealed that invasive mucinous adenocarcinomas were overrepresented (Figure 1f). It is currently unknown whether the reactivity of these tumors represents true full-length ROS1 overexpression or a nonspecific technical artifact perhaps associated with abundant mucin. In any event, histologic appearance should help determine the likelihood of *ROS1* rearrangement because invasive mucinous adenocarcinomas are typically associated with *KRAS* mutation[20] that hardly coexists with *ROS1* rearrangement. Only one invasive mucinous adenocarcinoma with *ROS1* rearrangement has been reported to our knowledge.[5]

There were 2 *ROS1*-rearranged tumors that exhibited less staining than the remaining 15 cases. Case P8 was almost purely composed of signet-ring

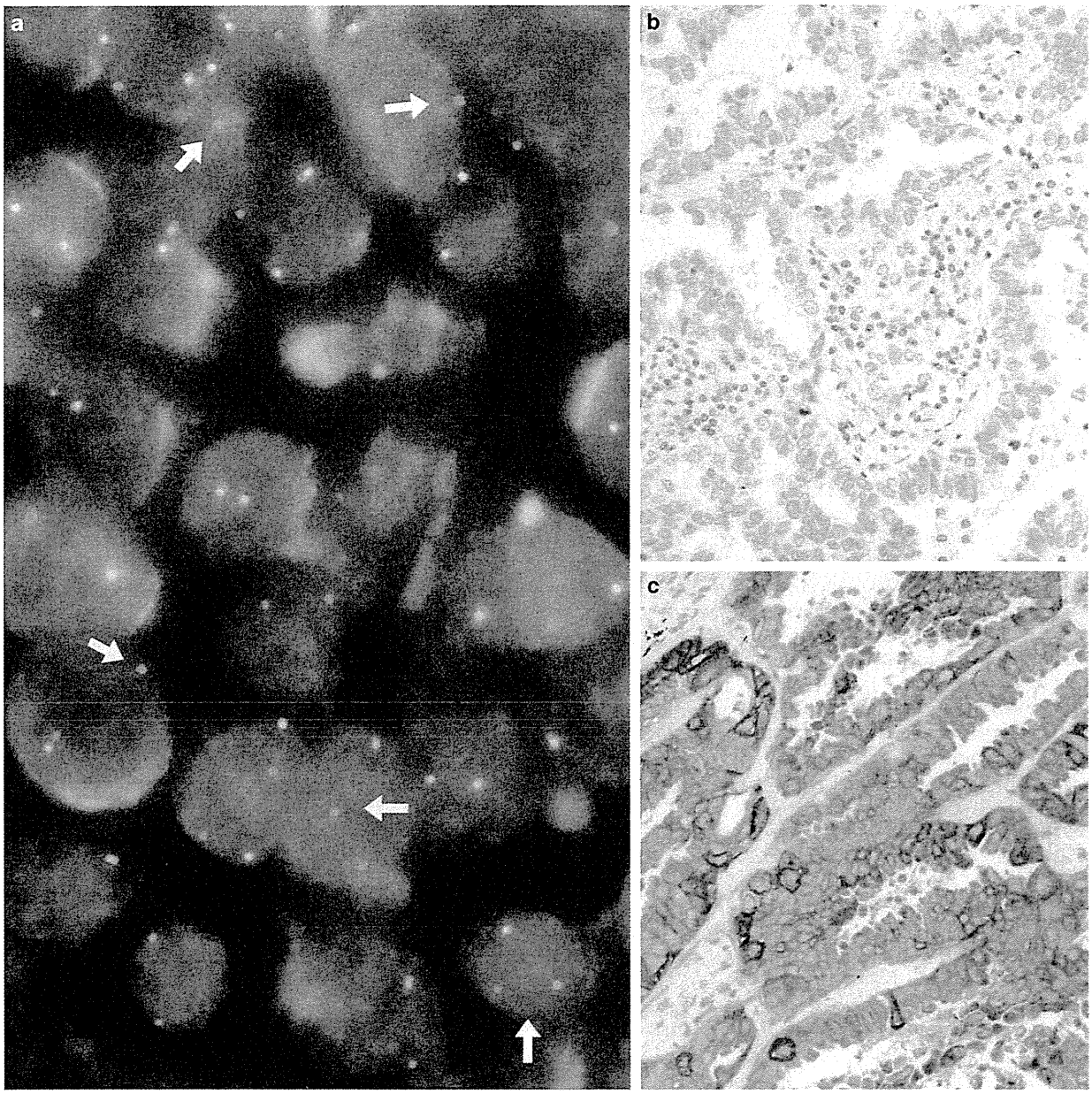

Figure 5 One case showed *ROS1* rearrangement determined using FISH (**a**, arrows indicate rearranged signals), although no *ROS1* fusion transcript was amplified using multiplex RT-PCR. ROS1 immunostaining was almost negative (**b**). The tumor harbored an *EGFR* exon 19 deletion and diffusely expressed mutant EGFR as detected using immunohistochemistry (**c**).

cells and reminds us of a reported pitfall of ALK immunohistochemistry for *ALK*-rearranged lung cancers that the staining can be reduced in signet-ring cells.[25] Although further study is needed, the potential decrease in immunoreactivity associated with signet-ring cells warrants recognition, particularly because signet-ring cell morphology is characteristic of *ROS1*-rearranged lung cancer.[8]

The other outlier case (P17) posed a greater challenge to interpret because its driver gene status was not clear. Although FISH analysis indicated gene rearrangement, multiplex RT-PCR did not amplify a *ROS1*-fusion product. Of note, this was the only case in which a discrepancy occurred between FISH and RT-PCR, of all the cases investigated in the present study as well as in our previous study[8] on *ROS1*-rearranged lung cancers. Although one may explain this discordance by hypothesizing a fusion partner that is not covered by the present RT-PCR design, the very low ROS1 immunoreactivity (H-score = 5), unlike all other *ROS1*-rearranged cases, casts doubt on the oncological relevance of *ROS1* rearrangement. The presence of an *EGFR* mutation and diffuse strong overexpression of a

mutant EGFR in this case further suggest that the tumor is predominantly addicted to the EGFR signaling with only a minor, if any, contribution from ROS1 activity. Only rarely does *ROS1* rearrangement coexist with *EGFR* mutations in lung cancers, and two cases with such a genotype have been reported to show immunohistochemical coexpression of ROS1 and mutant EGFR.[9] The present case is, instead, reminiscent of two ALK-immunonegative adenocarcinomas reported by Sasaki *et al*[26] that harbored an *ALK*-rearrangement (confirmed by FISH) and an *EGFR* mutation. Future studies such as those using comprehensive sequencing methods may clarify the underlying mechanism that accounts for these unusual disparities. If this case P17 were excluded from the *ROS1*-rearranged cohort, the sensitivity of ROS1 immunohistochemistry would reach 100% by using the criteria that we have proposed (that is, H-score ≥ 150, extent $\geq 75\%$, or intensity $\geq 2+$).

In summary, our present results agree with those reported by Rimkunas *et al*[9] in that ROS1 immunohistochemistry by using a newly developed antibody is useful for screening of lung cancer patients for molecular therapy. However, as full-length ROS1 is expressed in a proportion of *ROS1*-non-rearranged cases, establishment of optimal interpretative criteria is critical to achieve concordance with genetic status. High H-score ($\geq$ 150), diffuse extent, or moderate-to-strong staining intensity provide helpful clues to predict *ROS1* rearrangement. Globular reactivity and plasma membranous accentuation correlate with *CD74* and *EZR* as fusion partners, and these patterns are likely to be fusion-specific. Although ROS1 immunohistochemistry is unlikely to replace confirmatory molecular assays, we expect that it will become an integral part of diagnostic algorithm in thoracic oncology. For example, if ROS1 immunostaining is negative or only focally positive, such a case will be almost certainly negative for *ROS1* rearrangement, thus precluding the need of molecular analysis. In contrast, if a diffuse-positive staining is observed, particularly with a moderate–strong intensity, the possibility of *ROS1* rearrangement is high and the case should be sent for molecular confirmation. We further suspect that ROS1 immunohistochemistry may find additional utility in wider clinical field in the future because *ROS1* rearrangements have also been reported in a growing number of non-pulmonary tumors.[19,27,28]

Acknowledgments

We thank Sachiko Miura, Chizu Kina, Yuko Adegawa, and Ryosuke Yamaga for their superb technical assistance. This work was supported in part by the Program for Promotion of Fundamental Studies in Health Sciences from the National Institute of Biomedical Innovation (NIBIO), Grants-in-Aid from the Ministry of Health, Labour and Welfare for the 3rd-term Comprehensive 10-year Strategy for Cancer Control, and the National Cancer Center Research and Development Fund. The National Cancer Center Biobank is supported by the National Cancer Center Research and Development Fund, Japan.

Disclosure/conflict of interest

The authors declare no conflict of interest.

References

1 Sawabata N, Asamura H, Goya T, *et al.* Japanese Lung Cancer Registry Study: first prospective enrollment of a large number of surgical and nonsurgical cases in 2002. J Thorac Oncol 2010;5:1369–1375.
2 Kwak EL, Bang YJ, Camidge DR, *et al.* Anaplastic lymphoma kinase inhibition in non-small-cell lung cancer. N Engl J Med 2010;363:1693–1703.
3 Lynch TJ, Bell DW, Sordella R, *et al.* Activating mutations in the epidermal growth factor receptor underlying responsiveness of non-small-cell lung cancer to gefitinib. N Engl J Med 2004;350:2129–2139.
4 Rikova K, Guo A, Zeng Q, *et al.* Global survey of phosphotyrosine signaling identifies oncogenic kinases in lung cancer. Cell 2007;131:1190–1203.
5 Bergethon K, Shaw AT, Ou SH, *et al.* ROS1 rearrangements define a unique molecular class of lung cancers. J Clin Oncol 2012;30:863–870.
6 Davies KD, Le AT, Theodoro MF, *et al.* Identifying and targeting ROS1 gene fusions in non-small cell lung cancer. Clin Cancer Res 2012;18:4570–4579.
7 Takeuchi K, Soda M, Togashi Y, *et al.* RET, ROS1 and ALK fusions in lung cancer. Nat Med 2012;18:378–381.
8 Yoshida A, Kohno T, Tsuta K, *et al.* ROS1-rearranged lung cancer: a clinicopathologic and molecular study of 15 surgical cases. Am J Surg Pathol 2013;37:554–562.
9 Rimkunas VM, Crosby K, Kelly M, *et al.* Analysis of receptor tyrosine kinase ROS1 positive tumors in non-small cell lung cancer: identification of a FIG-ROS1 fusion. Clin Cancer Res 2012;18:4449–4457.
10 Suehara Y, Arcila M, Wang L, *et al.* Identification of KIF5B-RET and GOPC-ROS1 fusions in lung adenocarcinomas through a comprehensive mRNA-based screen for tyrosine kinase fusions. Clin Cancer Res 2012;18:6599–6608.
11 Govindan R, Ding L, Griffith M, *et al.* Genomic landscape of non-small cell lung cancer in smokers and never-smokers. Cell 2012;150:1121–1134.
12 Seo JS, Ju YS, Lee WC, *et al.* The transcriptional landscape and mutational profile of lung adenocarcinoma. Genome Res 2012;22:2109–2119.
13 Arai Y, Totoki Y, Takahashi H, *et al.* Mouse model for ROS1-rearranged lung cancer. PLoS One 2013;8:e56010.
14 Shaw A, Camidge D, Engelman J, *et al.* Clinical activity of crizotinib in advanced non-small cell lung cancer (NSCLC) harboring ROS1 gene rearrangement. J Clin Oncol 2012;30:Suppl; abstr 7508.
15 Li C, Fang R, Sun Y, *et al.* Spectrum of oncogenic driver mutations in lung adenocarcinomas from East Asian never smokers. PLoS One 2011;6:e28204.

16 Acquaviva J, Wong R, Charest A. The multifaceted roles of the receptor tyrosine kinase ROS in development and cancer. Biochim Biophys Acta 2009;1795: 37–52.
17 Lee HJ, Seol HS, Kim JY, *et al.* ROS1 receptor tyrosine kinase, a druggable target, is frequently overexpressed in non-small cell lung carcinomas via genetic and epigenetic mechanisms. Ann Surg Oncol 2013;20: 200–208.
18 Fukui T, Ohe Y, Tsuta K, *et al.* Prospective study of the accuracy of EGFR mutational analysis by high-resolution melting analysis in small samples obtained from patients with non-small cell lung cancer. Clin Cancer Res 2008;14:4751–4757.
19 Charest A, Lane K, McMahon K, *et al.* Fusion of FIG to the receptor tyrosine kinase ROS in a glioblastoma with an interstitial del(6)(q21q21). Genes Chromosomes Cancer 2003;37:58–71.
20 Travis WD, Brambilla E, Noguchi M, *et al.* International Association for the Study of Lung Cancer/ American Thoracic Society/European Respiratory Society International multidisciplinary classification of lung adenocarcinoma. J Thorac Oncol 2011;6: 244–285.
21 Camidge DR, Kono SA, Flacco A, *et al.* Optimizing the detection of lung cancer patients harboring anaplastic lymphoma kinase (ALK) gene rearrangements potentially suitable for ALK inhibitor treatment. Clin Cancer Res 2010;16:5581–5590.
22 Yatabe Y, Matsuo K, Mitsudomi T. Heterogeneous distribution of EGFR mutations is extremely rare in lung adenocarcinoma. J Clin Oncol 2011;29: 2972–2977.
23 Stumptner-Cuvelette P, Benaroch P. Multiple roles of the invariant chain in MHC class II function. Biochim Biophys Acta 2002;1542:1–13.
24 Bruce B, Khanna G, Ren L, *et al.* Expression of the cytoskeleton linker protein ezrin in human cancers. Clin Exp Metastasis 2007;24:69–78.
25 Murakami Y, Mitsudomi T, Yatabe Y. A screening method for the ALK fusion gene in NSCLC. Front Oncol 2012;2:24.
26 Sasaki T, Koivunen J, Ogino A, *et al.* A novel ALK secondary mutation and EGFR signaling cause resistance to ALK kinase inhibitors. Cancer Res 2011;71: 6051–6060.
27 Lee J, Lee SE, Kang SY, *et al.* Identification of ROS1 rearrangement in gastric adenocarcinoma. Cancer 2013;119:1627–1635.
28 Gu TL, Deng X, Huang F, *et al.* Survey of tyrosine kinase signaling reveals ROS kinase fusions in human cholangiocarcinoma. PLoS One 2011;6:e15640.

PLOS ONE

Mouse Model for ROS1-Rearranged Lung Cancer

Yasuhito Arai[1☯], Yasushi Totoki[1☯], Hiroyuki Takahashi[1], Hiromi Nakamura[1], Natsuko Hama[1], Takashi Kohno[2], Koji Tsuta[3], Akihiko Yoshida[3], Hisao Asamura[4], Michihiro Mutoh[5], Fumie Hosoda[1], Hitoshi Tsuda[3], Tatsuhiro Shibata[1]*

1 Division of Cancer Genomics, National Cancer Center Research Institute, Chuo-ku, Tokyo, Japan, **2** Division of Genome Biology, National Cancer Center Research Institute, Chuo-ku, Tokyo, Japan, **3** Division of Pathology and Clinical Laboratories, National Cancer Center Hospital, Chuo-ku, Tokyo, Japan, **4** Thoracic Surgery Division, National Cancer Center Hospital, Chuo-ku, Tokyo, Japan, **5** Division of Cancer Prevention Research, National Cancer Center Research Institute, Chuo-ku, Tokyo, Japan

Abstract

Genetic rearrangement of the *ROS1* receptor tyrosine kinase was recently identified as a distinct molecular signature for human non-small cell lung cancer (NSCLC). However, direct evidence of lung carcinogenesis induced by *ROS1* fusion genes remains to be verified. The present study shows that *EZR-ROS1* plays an essential role in the oncogenesis of NSCLC harboring the fusion gene. *EZR-ROS1* was identified in four female patients of lung adenocarcinoma. Three of them were never smokers. Interstitial deletion of 6q22–q25 resulted in gene fusion. Expression of the fusion kinase in NIH3T3 cells induced anchorage-independent growth *in vitro*, and subcutaneous tumors in nude mice. This transforming ability was attributable to its kinase activity. The ALK/MET/ROS1 kinase inhibitor, crizotinib, suppressed fusion-induced anchorage-independent growth of NIH3T3 cells. Most importantly, established transgenic mouse lines specifically expressing EZR-ROS1 in lung alveolar epithelial cells developed multiple adenocarcinoma nodules in both lungs at an early age. These data suggest that the *EZR-ROS1* is a pivotal oncogene in human NSCLC, and that this animal model could be valuable for exploring therapeutic agents against *ROS1*-rearranged lung cancer.

Citation: Arai Y, Totoki Y, Takahashi H, Nakamura H, Hama N, et al. (2013) Mouse Model for ROS1-Rearranged Lung Cancer. PLoS ONE 8(2): e56010. doi:10.1371/journal.pone.0056010

Editor: John D. Minna, Univesity of Texas Southwestern Medical Center at Dallas, United States of America

Received October 3, 2012; **Accepted** January 4, 2013; **Published** February 13, 2013

Funding: This study was supported by the Program for Promotion of Fundamental Studies in Health Sciences from the National Institute of Biomedical Innovation, National Cancer Center Research and Development Funds (23-A-7 and 23-B-28), Research Grant of the Princess Takamatsu Cancer Research Fund and Grants-in-Aid from the Ministry of Health, Labour and Welfare for the 3rd-term Comprehensive 10-year Strategy for Cancer Control. National Cancer Center Biobank is supported by the National Cancer Center Research and Development Fund, Japan. The funders had no role in study design, data collection and analysis, decision to publish, or preparation of the manuscript.

Competing Interests: The authors have declared that no competing interests exist.

* E-mail: tashibat@ncc.go.jp

☯ These authors contributed equally to this work.

Introduction

Lung cancer is the leading cause of cancer death around the world [1]. Lung adenocarcinoma (LADC), the most common form of non-small-cell lung cancer (NSCLC), comprises several different genomic subsets defined by unique oncogenic alterations, and a considerable proportion of LADC cases harbor driver alterations in the *EGFR*, *KRAS* and *ALK* genes at the mutually exclusive manner with rare exceptions [2–5]. Understanding the molecular basis of cancer allows us to develop therapeutic agents that target genetic druggable aberrations identified in cancer genomes. Tyrosine kinase inhibitors (TKIs) that target the EGFR and ALK proteins are particularly effective in the treatment of LADC carrying *EGFR* mutations and *ALK* fusions, respectively [2–6]. However, the development of an effective TKI requires experimental validation of the genetic aberrations as actionable and druggable. Transgenic mouse models harboring *EGFR* mutations or *EML4-ALK* gene fusions have successfully demonstrated the oncogenic potential of the alterations and the efficacy of TKI therapy [7,8]. Genetic rearrangement of the *ROS1* was recently identified as a distinct molecular signature for human LADC [9–16]. In the present study, we established a mouse model of *ROS1* fusion, and showed that *EZR-ROS1* as an essential driver oncogene in lung carcinogenesis.

Results

Identification of EZR-ROS1 Fusion Gene in LADC of Never-smokers

Whole transcriptome high-throughput sequencing of tumor specimens is one of the most effective methods for identifying fusion oncogenes [17]. Analysis of five LADC cases of never-smokers without *EGFR/KRAS/ALK* alterations using transcriptome sequencing identified 56 reads overriding the in-frame *EZR-ROS1* gene fusion point connecting *EZR* exon 10 to *ROS1* exon 34 in one tumor. RT-PCR analysis of matched non-cancerous tissues confirmed tumor-specific expression of the fusion transcript (Figure 1A). In addition, transcriptome sequencing clearly demonstrated a specific increase in the expression of the fused 3′ portion of *ROS1* (exons 34 to 43) after the breakpoint, suggesting that the *EZR-ROS1* fusion transcript causes aberrant overexpression of *ROS1* tyrosine kinase domain along with the 5′ portion of *EZR* (Figure 1B). SNP array comparative genomic hybridization (array CGH) data showed that this fusion gene was generated by a large interstitial deletion spanning ~41.5 Mb on chromosome 6q22-q25 (Figure 1C). Genomic PCR and sequencing analysis also revealed the deletion of 41.5 Mb causing somatic fusions of the

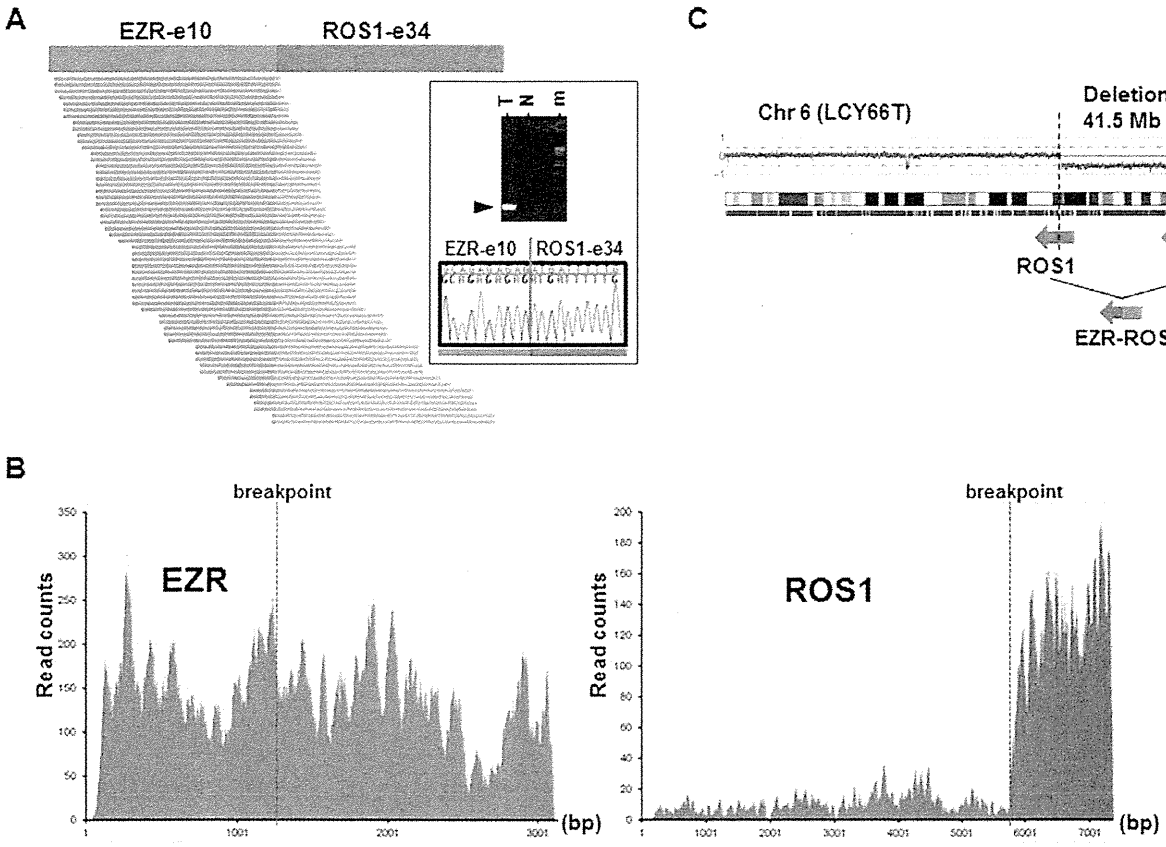

Figure 1. Identification of the *EZR-ROS1* fusion. (A) Junction reads representing *EZR-ROS1* fusion transcripts in LCY66T sample (left). Sanger sequencing of the RT-PCR product validated tumor-specific in-frame fusion transcript (right). m: molecular marker. (B) Expression profiles of *EZR* and *ROS1* in LCY66T. Active expression of the *ROS1* gene was observed after the fusion point. (C) SNP array CGH analysis of the LCY66T. Copy number throughout chromosome 6 is plotted as the log2 ratio.
doi:10.1371/journal.pone.0056010.g001

EZR intron 10 at 6q25 with the *ROS1* intron 33 at 6q22 (Figure S1).

RT-PCR and Sanger sequencing analysis of 569 LADC specimens from Japanese individuals, including the above-mentioned cases (343 cases with early pathological stage and 226 cases with advanced stage), identified four cases harboring this fusion transcript (Figure S2). All four *EZR-ROS1* fusion-positive cases were female, and harbored neither *EGFR/KRAS/HER2* mutations nor *EML4-ALK/KIF5B-RET* fusions. Three cases were poorly differentiated adenocarcinomas of never smokers, and the other was a moderately differentiated adenocarcinoma of a smoker.

Transforming Activity of EZR-ROS1

EZR-ROS1 cDNA isolated from the tumor specimen encoded a protein of 858 amino acids (Figure 2A; GenBank/DDBJ accession number AB698667). The protein connects the FERM domain [18] of ezrin (EZR) with the transmembrane and kinase domains of ROS1, but lacks most of the coiled-coil domain of EZR.

To examine the oncogenic activity of the *EZR-ROS1* fusion *in vitro*, we established stable NIH3T3 clones expressing wild-type EZR-ROS1 and kinase-dead mutant EZR-ROS1 (KD), in which the ATP-binding lysine residue was mutated to methionine (K491M), as well as mutants with serially deleted amino-terminal FERM domains (DL1, DL2 and DL3; Figure 2A). Autophosphorylation of specific tyrosine residues is a crucial event in the activation of distinct signal transduction pathways, and Tyr-2274 of ROS1 is a specific autophosphorylation site essential to induce kinase activity for transformation [19]. In transformation assays, phosphorylation of the Tyr-2274 (corresponding to Tyr-785 in wild type EZR-ROS1 fusion) was observed in a wild-type EZR-ROS1-expressing clone, but was not detected in kinase-dead (KD) and deleted (DL) mutants; this implies that the amino-terminal portion of FERM (1–88 amino acids) is necessary for ROS1 kinase activation (Figure 2B). Wild-type *EZR-ROS1* but not KD/DL mutants specifically induced activation of STAT3 for downstream signaling, and produced significantly anchorage-independent growth (Figure 2C, D). The anchorage-independent growth induced by *EZR-ROS1* was suppressed by treatment with crizotinib, a TKI against ALK/MET/ROS1, whereas the growth induced by another oncogene of lung, *CCDC6-RET* [11] was not (Figure 2E). On the contrary, vandetanib, a TKI against RET/EGFR/VEGFR was effective in inhibiting the colony formation of CCDC6-RET expressing cells, but not in the EZR-ROS1 expressing cells. As shown in Figure 2C, crizotinib treatment suppressed phosphorylation of EZR-ROS1, and inhibit the activation of STAT3.

Next, the NIH3T3 cells were subcutaneously injected into immune-compromised mice. Wild-type EZR-ROS1-expressing clones invariably produced tumors (6/6), while none of the KD

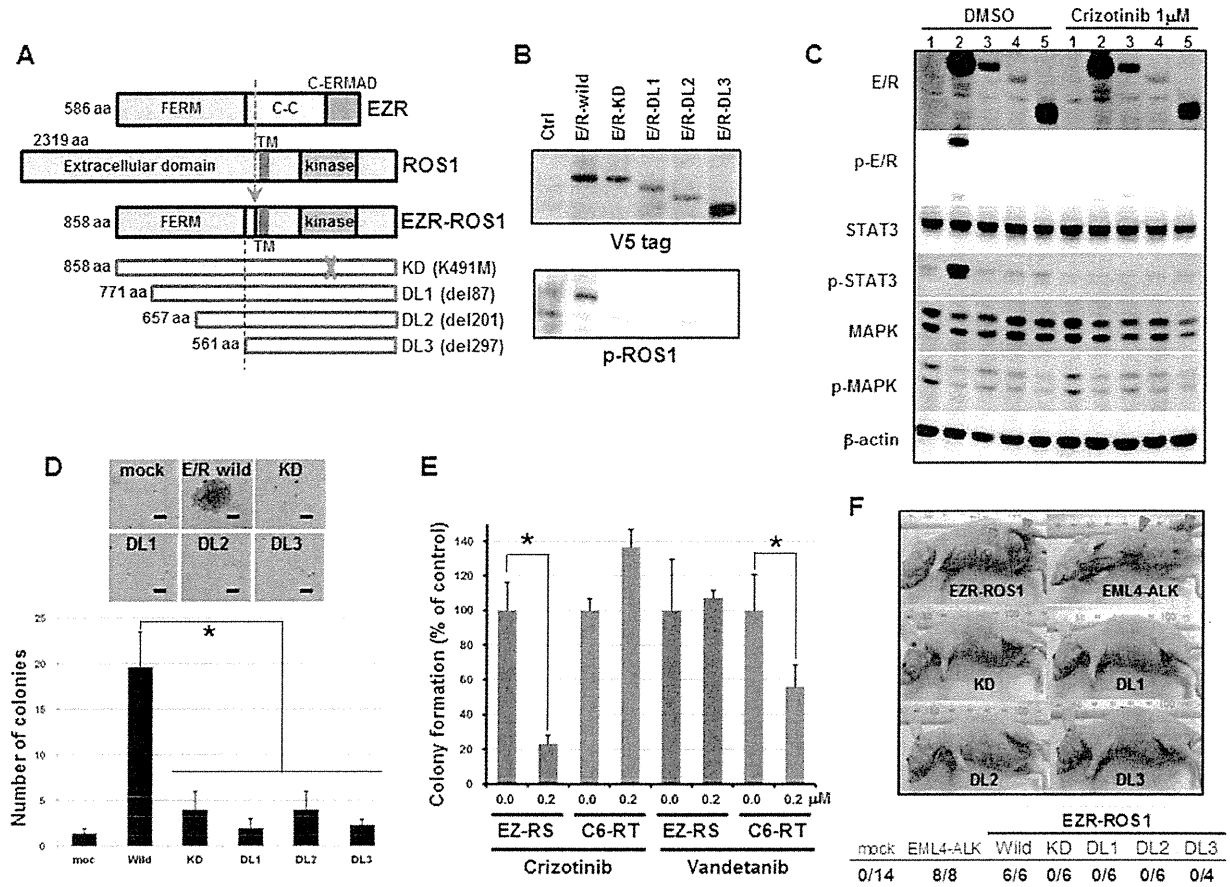

Figure 2. Oncogenic activity of the *EZR-ROS1* fusion gene. (A) Schematic representation of EZR, ROS1, EZR-ROS1, and deletions/mutations of EZR-ROS1 genes. The domain organization is shown. C-C: coiled-coil domain; TM: transmembrane; C-ERMAD: C-terminal ERM associated domain. (B) ROS1 phosphorylation in wild-type and mutant EZR-ROS1 (E/R)-expressing NIH3T3 clones. Cell lysates from each clone were immunoblotted with anti-V5-tag (top) and anti-phosphorylated ROS1 (Tyr-2274, bottom) antibodies. (C) Suppression of ROS 1 kinase activity of EZR-ROS1 by crizotinib inhibits STAT3 activation. NIH3T3 cells transfected with 1: empty vector, 2: wild-type EZR-ROS1, 3: KD 4: DL1, 5: DL3 were serum starved and treated for 2 hr with DMSO or 1 μM of crizotinib, and immunoblotted with the relevant antibodies. β-actin was used as a loading control. E/R: EZR-ROS1, p-E/R: phosphorylated EZR-ROS1 detected with an anti-phosphotyrosine-2274 antibody of ROS1. (D) Soft agar colony formation of wild-type and mutant EZR-ROS1 expressing NIH3T3 clones. A representative picture of colony formation for each clone is plotted at the top (scale bar, 100 μm). The number of colonies obtained for each clone is plotted at the bottom. *P<0.05. (E) Crizotinib-induced suppression of anchorage-independent growth of NIH3T3 cells expressing EZR-ROS1. Bar graph showing the percentage of NIH3T3 colonies induced by *EZR-ROS1* or *CCDC6-RET* after treatment with 200 nM of crizotinib or vandetanib with respect to those formed by DMSO-treated cells. EZ-ROS: EZR-ROS1, C6-RET: CCDC6-RET. *P<0.05. (F) Representative pictures of mice subcutaneously transplanted with NIH3T3 cells expressing wild-type, kinase domain-mutated, or amino-terminal-deleted EZR-ROS1. An EML4-ALK-expressing NIH3T3 clone was used as a positive control. The number of tumors per injection in each transfectant is shown below the photographs.
doi:10.1371/journal.pone.0056010.g002

and DL mutants-expressing clones produced tumors (Figure 2F), confirming that *in vivo* tumorigenic activity of *EZR-ROS1* requires ROS1 kinase activity.

Development of LADC in EZR-ROS1 Transgenic Mice

To further evaluate the role of *EZR-ROS1* in lung carcinogenesis, we generated transgenic mice expressing the fusion gene under the control of a type 2 alveolar epithelium-specific surfactant C gene promoter [20] (Figure 3A). We obtained four independent lines (TgA, B, C and D) with different copy number of the transgene (Figure S3) and detected lung adenocarcinoma nodules in all lines examined except TgD. Analysis of fusion protein expression level among them revealed no expression in TgD (Figure S4). The birth rate of transgene-positive progenies was low in TgC (Transgene-positive F1 progeny number : total F1 number; 1:3), and we failed to keep up a TgC line, then we mainly analyzed one line (TgA), which harbors approximately four copies of the transgene. RT-PCR and immunoblot analysis verified lung-specific *EZR-ROS1* mRNA and protein expression, and indicated phosphorylation of the EZR-ROS1 fusion protein (Figure 3B). Although endogenous *Ezrin* was ubiquitously expressed in many tissues, endogenous *Ros1*-transcript was detected only in stomach, kidney and lung. Protein expression levels of endogenous ROS1 were very weak compared with the levels of the fusion gene in the transgenic mice (Figure S4). Even at the four-week-old, multiple lesions over 1 mm in diameter were detected in the transgenic mice, and tumors occupied over 40% of sectioned surface of lung (Figure 3C and Figure S5). Computed tomography examination